Advancements in cancer imaging: receptor-targeted approaches for enhanced precision and therapy guidance

Rezaei, S.

Chapter 4

Expression of Cholecystokinin 2 Receptor (CCK2R) in Rectal Cancer: Clinical Relevance and In Vitro Targeting with a Fluorescent CCK2R-Binding Peptide

Somayeh Rezaei, Xi Zhang, Ronald L.P. van Vlierberghe, Amber Piet, Elma Meershoek-Klein Kranenbarg, Ajinkya Manelkar, Yann Seimbille, Peter Laverman, Louise van der Weerd, Alexander L. Vahrmeijer, and Peter J.K. Kuppen. Z

Pharmacological Research Reports
December 2025, 4: 100054. 10.1016/j.prerep.2025.100054

Abstract

The cholecystokinin type 2 receptor (CCK2R), which mediates the effects of gastrin and cholecystokinin (CCK), is known to promote colorectal cancer (CRC) proliferation in advanced stages. Though well-studied in gastric and pancreatic cancers, the role of CCK2R in colorectal, especially rectal cancer (RC), is still emerging. In this research, we initially evaluated CCK2R expression across rectal and colorectal cancer cell lines using qRT-PCR to establish baseline expression patterns. To explore the potential for near-infrared (NIR) fluorescence-based tumor targeting, we synthesized a CCK2R-binding peptide conjugate, Cy5@PP-F11, and demonstrated its receptor-specific uptake in vitro through live-cell imaging microscopy. While these results suggest promise for tumor targeting, further studies are needed to assess its *in vivo* performance and utility in fluorescence-guided surgery. In addition, a cohort of 495 Stage I-IV rectal cancer patients was analyzed using tissue microarrays (TMAs) and immunohistochemistry (IHC) to assess CCK2R expression in both tumor and normal tissues. Expression patterns and their prognostic significance were evaluated in relation to clinicopathological parameters. CCK2R localization and expression levels were quantified in both the epithelial and stromal tumor compartments, with cytoplasmic and nuclear staining specifically analyzed in the epithelial compartment. Scoring data were assessed to determine their clinical relevance. Our findings revealed significant overexpression of CCK2R in both epithelial and stromal compartments of rectal cancer tissues compared to normal tissues, showing its high suitability as target for tumor imaging. While epithelial CCK2R expression showed no significant link to clinical staging, stromal expression was notably involved, indicating a role in tumor-stroma interactions and the tumor microenvironment.

1. Introduction

Colorectal cancer (CRC) accounted for an estimated 1.9 million new cases and 904,000 deaths in 2022, representing nearly one in every 10 cancer cases and deaths worldwide [1] Rectal cancer constitutes approximately 30% of all colorectal cancer cases [2]. These cancers typically originate in the mucosal lining of the colon or rectum, often beginning as benign adenomatous polyps, which can progressively transform into malignant tumors over time if left untreated [3]. While colon and rectal cancers share many genetic and molecular traits, they differ in treatment approaches and outcomes due to anatomical and physiological distinctions [4]. Early detection through screening methods, like colonoscopy and fecal occult blood tests, has proven effective in reducing CRC mortality, as early-stage cancers often have a favorable prognosis [5]. Current treatments for rectal cancer include local excision, surgery, chemotherapy, and radiotherapy. Local excision and surgery are effective for localized cases but challenging in advanced stages. Chemotherapy and radiotherapy help shrink tumors but carry significant side effects. For advanced disease, these therapies are often palliative, highlighting the need for improved options [6].

The cholecystokinin 2 receptor (CCK2R), a member of the G protein-coupled receptor (GPCR) family, interacts with the ligands gastrin and cholecystokinin (CCK), both of which are critical growth factors in gastrointestinal tissues and central nervous system [7]. Elevated levels of gastrin have been demonstrated to specifically promote cancer cell proliferation through CCK2R, rather than through cholecystokinin 1 receptor (CCK1R) [8]. CCK1R is more expressed than CCK2R in esophageal and colon cancers, and CCK1R antagonists inhibit colon cancer cell growth, though its clinical relevance remains uncertain [9]. CCK2R is primarily expressed in the brain and, to a lesser extent, in the gastric mucosa, where it remains largely inaccessible to parenterally administered drugs. In contrast, CCK2R and its splice variants are significantly overexpressed in a range of malignancies, including gastric adenocarcinoma, medullary thyroid carcinoma, colorectal, pancreatic, ovarian, and small cell lung cancers, as well as tumors of the brain, stomach, and gastrointestinal stroma [7, 10]. Approximately 27 % of CRC cases exhibit CCK2R positivity, with elevated CCK2R expression significantly associated with adverse prognostic outcomes. Research indicates that aberrant CCK2R expression correlates with specific histological subtypes, particularly mucinous carcinoma (MCA), where overexpression of CCK2R is frequently observed [11]. Furthermore, inactivation of CCK2R has been shown to suppress colonic crypt fission, cellular proliferation, and ultimately the progression of colorectal cancer [12].

Accurate, real-time detection of tumors and critical structures during surgery remains a challenge[13]. Tumor-targeting ligands can be conjugated to near-infrared (NIR, 700–900 nm) fluorophores, enabling real-time visualization of tumors during surgery with specialized imaging systems. NIR fluorescence penetrates up to 8 mm into tissue, allowing detection of partially hidden targets[14]. Several NIR fluorophore-labeled ligands, including antibodies, are in clinical trials. Antibodies have high target specificity but may cause immune reactions and slow clearance, while peptides offer better pharmacokinetics but lower target affinity [15]. PP-F11 is a gastrin analog optimized for targeting CCK2R [16, 17]. Radiolabeled PP-F11 variants exhibit excellent biodistribution with favorable tumor-to-background activity ratios, including high tumor-to-kidney uptake ratios, as validated in preclinical and initial human studies [17, 18]. The high receptor specificity, improved metabolic stability, reduced renal retention, and favorable tumor-to-kidney uptake ratios of PP-F11 and its derivatives make them promising candidates for diagnostic imaging and therapy in CCK2R-expressing cancers [16, 18]. In this

study, we investigated Cyanine 5 labeled PP-F11 (Cy5@PP-F11) as a fluorescent probe to enhance tumor-imaging and improve the targeting of CCK2R-expressing cells, with the goal of providing precise intraoperative guidance during surgery. Additionally, we analyzed a cohort of rectal cancer patients to evaluate CCK2R expression in both epithelial and stromal compartments and its clinical relevance.

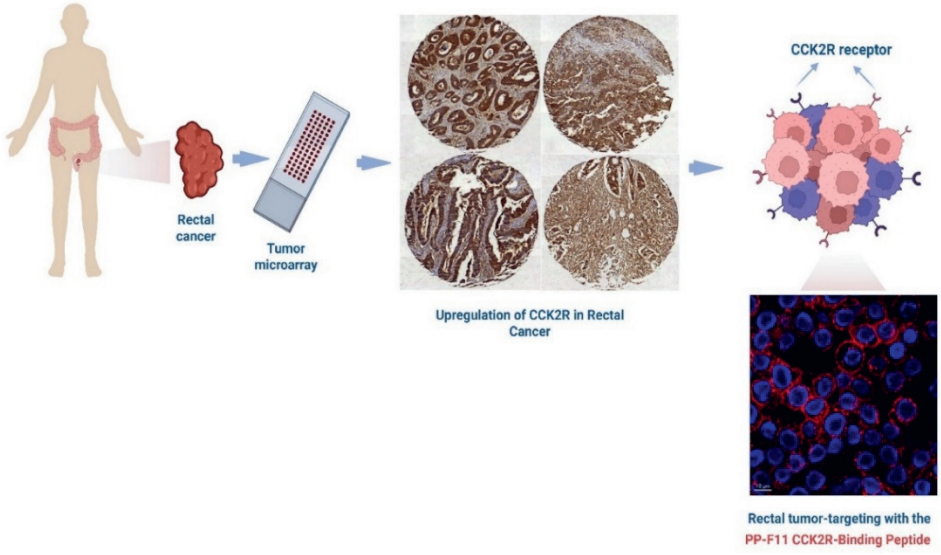

Scheme 1. Schematic illustration showing the upregulation of Cholecystokinin 2 receptor (CCK2R) in rectal cancer and the molecular imaging of rectal cancer using PP-F11 CCK2R-binding peptide.

2. Experimental section

Peptides. The cholecystokinin 2 receptor (CCK2R) targeting peptide, PP-F11, was modified to enhance its functionality for imaging applications. The resulting peptide, Cy5-$(GABOB)_2$-β-Ala-Trp-(N-Me)Nle-Asp-1-Nal-NH_2 (Cy5@PP-F11), includes a Cyanine 5 (Cy5) near-infrared fluorescent dye for imaging and $(GABOB)_2$-β-Ala spacers to improve solubility, stability, and flexibility. The peptide sequence is derived from compound 2, as reported in the [16], and was selected for its shorter and more efficient synthesis. The peptide was synthesized using standard Fmoc-based solid-phase peptide synthesis method, purified via high-performance liquid chromatography (HPLC), and characterized by electrospray mass spectrometry. All peptides were provided by the group of Dr. Yann Seimbille at Erasmus MC University, Netherlands. Comprehensive information on peptide synthesis and characterization is available in the Supplementary Materials.

Cell culture.

A431/CCK2R- and A431/Mock-transfected human epidermoid carcinoma cells, generously provided by Dr. Peter Laverman (Department of Medical Imaging, Nuclear Medicine, Radboud University

Medical Center, Nijmegen), were used in this study. A431-CCK2R cells were stably transfected with the CCK2 receptor, while A431-Mock cells were transfected with an empty vector. These cell lines were originally developed and characterized by Dr. Luigi Aloj, as previously described by Aloj et al.[19]. Additional cell lines included SW620 and HTC-15 (human colorectal adenocarcinoma), SW480, SW1116, and HT-29 (human colon carcinoma), Hra19 and SW1463 (human rectal adenocarcinoma), and OVCAR3 (human ovarian adenocarcinoma). Cells were cultured in Roswell Park Memorial Institute (RPMI) or Dulbecco's Modified Eagle Medium (DMEM), supplemented with 10% fetal bovine serum (FBS) and 100 U/mL penicillin/streptomycin (P/S), and maintained at 37°C in a 5% CO_2 atmosphere. A431-CCK2R and A431-Mock cells were specifically cultured in DMEM supplemented with 10% FBS, 5 µg/mL gentamicin, glutamine, and penicillin/streptomycin. All cell culture reagents, including FBS, penicillin/streptomycin, and media, were sourced from Gibco Laboratories (Thermo Scientific™, Waltham, MA, USA).

RNA expression level assay

CCK2R mRNA expression was evaluated using qRT-PCR across a range of tumor cell lines, including A431-CCK2R, A431-Mock, SW620, SW480, SW1116, Hra19, HTC-15, HT-29, SW1463, and OVCAR3. The cells were cultured in a 6-well plate until confluent and washed with ice-cold phosphate-buffered saline (PBS). RNA was isolated from the samples using the Nucleospin RNA isolation kit (Machery-Nagel, Düren, Germany) according to the manufacturer's instructions. RNA concentrations were determined using a Nanodrop 1000 spectrophotometer (Thermo Fisher Scientific). Complementary DNA (cDNA) was synthesized using the RevertAid First Strand cDNA Synthesis Kit with 1 µg of RNA input. The synthesized cDNA was then diluted to a concentration of 10 ng/µl for use in qPCR which was performed in triplicates using SYBR Green Master Mix (Bio-Rad Laboratories, Nazareth, Belgium) in a C1000 Touch Thermal Cycler with a CFX96 Optics Module (Bio-Rad). Primers used included forward CCK2R (GGGCACATTCATCTTTGGCACCG), forward β-actin (GCACAGAGCCTCGCCTT), reverse CCK2R (TGCAGTGGTCGGCAGATGGC), and reverse β-actin (GTTGTCGACGACGAGCG) at a concentration of 500 nM per PCR reaction. The specificity of all primers was confirmed by melting curve analysis, with an $r^2 > 0.98$. Gene quantification was performed relative to the housekeeping gene β-actin using the $2^{-}\Delta Cq$ method. Data analysis was conducted in Bio-Rad CFX Maestro 2.2 (version: 5.2.008.0222), and scatter plots were generated using GraphPad Prism 10 (version 10.2.3).

Live cell imaging microscopy

To evaluate the cellular localization of cell-bound Cy5@PP-F11, chamber slides were prepared with 50,000 cells per well from A431-CCK2R, A431-Mock, SW620, SW1116, Hra19, and SW1463 cell lines. The cells were cultured at 37°C in a 5% CO_2 atmosphere in cell culture media. After 24 hours (h), the cell culture medium was removed, and the cells were gently washed with fresh medium before staining with Hoechst (1:1000) for 15 minutes (min) at 4°C. Cells were then washed once with 1% BSA/PBS and treated with 50 nM or 100 nM of the Cy5@PP-F11 ligand at 4°C for 60 min. Following treatment, the cells were washed twice with 1% BSA/PBS. Each well was then filled with 300 µl of PBS before imaging. Imaging was performed using a Dragonfly 200 live cell imaging microscope.

Immunohistochemical analysis of CCK2R expression

To evaluate CCK2R expression, we performed immunohistochemical analysis following a rigorous protocol to ensure accuracy and reproducibility. Tissue sections (4-6 µm thick) were mounted on slides and dried overnight at 37°C. Deparaffinization was done with three 5-minute xylene incubations, followed by three rinses in absolute ethanol, and rehydration through 70% and 50% ethanol. Endogenous peroxidase activity was blocked by incubating the slides in a 0.3% H_2O_2 solution in PBS for 20 minutes. Antigen retrieval was achieved by heating the slides in a pH 6 buffer (EnVision FLEX Target Retrieval Solution Low pH (Dako, K8005) with the DAKO PT-link system. After two PBS washes, the slides were incubated overnight with an Anti-CCK2R antibody (16459-1-AP, Proteintech, Rosemont, USA) (1:600) in PBS with 1% BSA. The next day, unbound primary antibodies were removed by three PBS washes, and the slides were incubated with undiluted Envision/HRP secondary antibody for 30 minutes. Following three additional PBS washes, slides were developed using the Liquid DAB + Substrate Chromogen System (DAKO), following manufacturer's instructions. This results in a brown deposit at the location of the target antigen.

Study population

The study cohort was derived from the surgery only treatment arm of the Dutch TME trial (January 12, 1996, DUT-KWF-CKVO-9504, EORTC-40971, EU-96020), a multicenter trial conducted from 1996 to 1999. The study cohort was derived from the surgery only treatment arm of the Dutch TME trial (January 12, 1996, DUT-KWF-CKVO-9504, EORTC-40971, EU-96020), a multicenter trial conducted from 1996 to 1999. The trial was approved by the Leiden University Medical Center ethics committee (number 22/94-18).15 .This trial evaluated total mesorectal excision (TME) surgery with or without preoperative radiotherapy (5 × 5 Gray) [20]. Radiotherapy, surgical, and pathological procedures were standardized and quality-controlled. The trial and use of tissue samples were approved by the Medical Ethical Committee of Leiden University Medical Center, and written informed consent was obtained from all participants. A tissue microarray (TMA) was constructed with three representative tumor tissue punches for each patient using formalin-fixed, paraffin-embedded tumor samples from 496 patients with stage I–IV rectal cancer who underwent surgery without preoperative radiotherapy [19]. Additionally, TMAs of normal rectal tissues were included as controls.

CCK2R scoring methodology

The scoring of CCK2R expression was performed on each core of TME-TMA slides from both tumor and normal tissue samples. For each core, the percentage of the area (0–100%) occupied by epithelium or stromal regions was first determined. Within each region (epithelial or stromal), the percentage of cells stained with the CCK2R antibody (0–100%) was evaluated, followed by an assessment of the staining intensity. Staining intensity was graded on a four-point scale: 1 (Negative), 2 (Weak), 3 (Moderate), and 4 (Strong). Additionally, for the epithelial regions, staining localization was further categorized as cytoplasmic, nuclear, or both. For normal tissue sections, scoring was based solely on staining intensity (1: Negative, 2: Weak, 3: Moderate, and 4: Strong) and compared directly with tumor sections to evaluate differences. All tumor TME-TMA samples were analyzed using manual scoring in a double-blinded manner to ensure unbiased assessment.

Statistical analysis

GraphPad Prism 8.1.1 software (GraphPad Software, San Diego, CA, USA) was used for statistical analysis. Unless otherwise stated, all data are expressed as the mean ± standard deviation (SD) of 3 independent repeated experiments. The data were statistically significant by Student's *t*-test, unpaired, Mann-Whitney U test, and two-way analysis of variance (ANOVA). In all analyses, a *p*-value ≤ 0.05 was considered an indicator of statistical significance and is expressed as: # (not significant, P ≥ 0.05) * $p \leq 0.05$, ** $p \leq 0.01$, *** $p \leq 0.001$, **** $p \leq 0.0001$. Statistical analysis of the scoring data was performed using RStudio (version 4.4.2). Associations between CCK2R tumor epithelium or stroma expression, either percentage or intensity or percentage*intensity, and clinico-pathological variables were evaluated using the Student's t-test for continuous variables and the Chi-squared test for categorical variables. Survival outcomes were analyzed as follows: the primary outcome was Disease-Free Survival (DFS), defined as time from surgery to either disease relapse or death, whichever occurred first. The secondary outcome was Distant Recurrence-Free Survival (DRFS), which was defined as time from surgery to the first distant metastasis. Other patient outcome was Overall Survival (OS), defined as time from surgery to death from any cause. To determine the optimal cutoff for CCK2R expression, the MaxStat algorithm was applied to identify the threshold that best stratifies patients based on survival outcomes. This method systematically evaluates all possible cutoffs of a continuous variable and selects the threshold that yields the maximum standardized log-rank statistic, ensuring the most significant separation in survival outcomes. Patients were then categorized into high- and low-expression groups accordingly. Kaplan-Meier survival curves were generated, and differences between groups were assessed using the Log-rank test. Cox proportional hazards regression models were used for multivariate analyses to evaluate the association of CCK2R expression and other clinico-pathological variables with DFS, DRFS, and OS. Multivariate models included clinically relevant covariates to identify independent prognostic factors. Hazard ratios (HR) with 95% confidence intervals (CI) were reported. Statistical analyses were performed using R packages, including survival, survminer, and maxstat. A p-value < 0.05 was considered statistically significant.

3. Results

CCK2R expression was analyzed using qRT-PCR across various cell lines using the $2^{-}\Delta Ct$ method, normalized to the expression level of the β-actin gene (Figure 1). The positive control, the CCK2R-transfected cell line A431-CCK2R, exhibited significantly higher expression compared to all other cell lines (****$p \leq 0.0001$), while the negative control, A431−Mock, confirmed negligible baseline expression (Figure 1A). Among the colorectal and rectal cancer cell lines, including SW620, SW480, SW1116, HT29, HCT15, HRA19, and SW1463, CCK2R expression was consistently low, compare to A431-CCK2R with SW620 showing significantly higher levels than SW480, SW116, and HT29 (*p<0.05). HRA19 and SW1463 demonstrated intermediate expression levels, with notable differences compared to some other lines (*p<0.05 to ***p<0.001). OVCAR3, representing ovarian adenocarcinoma, exhibited low to moderate expression, significantly higher than HT29 but comparable to SW620 and SW1463 (Figure 1B). Next, based on the PCR data, six cell lines, including A431-CCK2R, SW620, SW1463, A431-Mock, SW1116, and HRA-19 were selected for live-cell imaging using the Cy5@PP-F11 peptide according to their relative CCK2R expression levels. We developed a novel peptide, Cy5@PP-F11 (Supplementary Figure 1), specifically developed to selectively target cells

expressing the CCK2R. To assess the binding specificity and cellular uptake of the Cy5@PP-F11 peptide, live cell imaging microscopy was used to visualize fluorescence signals in CCK2R-positive and -negative cell lines. Imaging revealed strong fluorescence localized in the cytoplasm of CCK2R-positive A431-CCK2R and SW620 cells, indicating effective binding and internalization of the Cy5@PP-F11 peptide (Figure 2). In contrast, CCK2R-negative A431-Mock, SW1116 and HRA19 cells exhibited minimal fluorescence, suggesting low nonspecific binding (Figure 3). Fluorescence intensity in CCK2R-positive cells was visually estimated to be 3-4 times higher than in negative controls, underscoring the selectivity of PP-F11 peptide for CCK2R-expressing cells. Strong intracellular fluorescence was observed in A431-CCK2R and SW620 cells, while minimal signal was detected in A431-Mock, SW1116, and HRA19 cells. Notably, the SW1463 cell line exhibited an intermediate level of fluorescence, indicating moderate CCK2R expression, which was higher than the negative controls but lower than A431-CCK2R and SW620 cells. This specificity is supported by the PCR data, which revealed significantly higher CCK2R mRNA expression in A431-CCK2R and SW620 cells compared to A431-Mock, SW1116, and HRA19 cells. The alignment between imaging and molecular expression underscores Cy5@PP-F11 as a highly effective probe for visualizing CCK2R-expressing tumors.

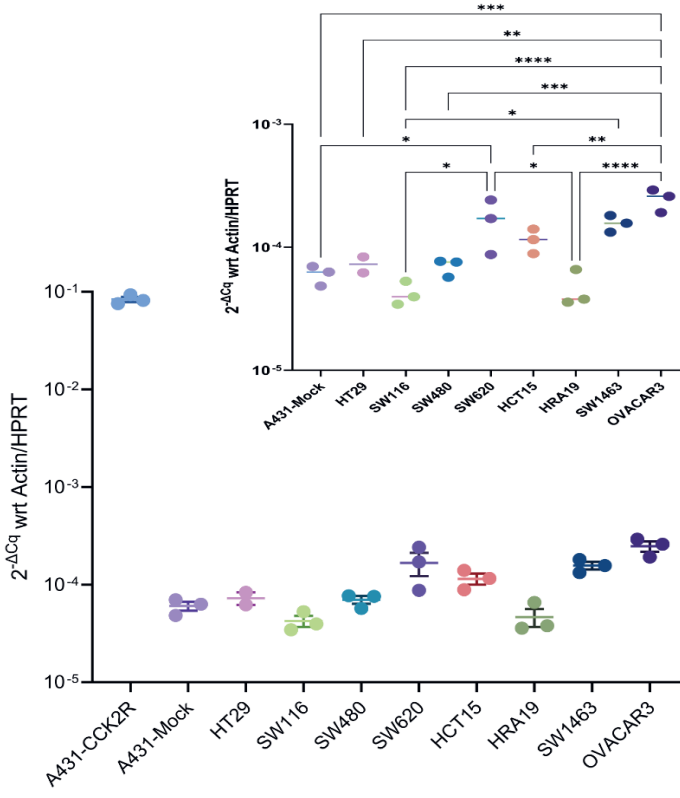

Figure 1. Relative Expression Analysis of CCK2R in different cell lines. Expression level (y-axis) was analyzed using qRT-PCR. **A)** Comparison of CCK2R expression across all cell lines (A431-CCK2R, A431-

Mock, HT29, SW116, SW480, SW620, HCT15, HRA19, SW1463, and OVACAR3) relative to A431+CCK2R (positive control) and A431-Mock (negative control). **B)** Detailed analysis of low-level CCK2R expression in colorectal, rectal, and ovarian cancer cell lines. Statistical significance is represented as: *p ≤ 0.05, **p ≤ 0.01, ***p ≤ 0.001, ****p ≤ 0.0001. Data are presented as mean ± SEM, n = 3.

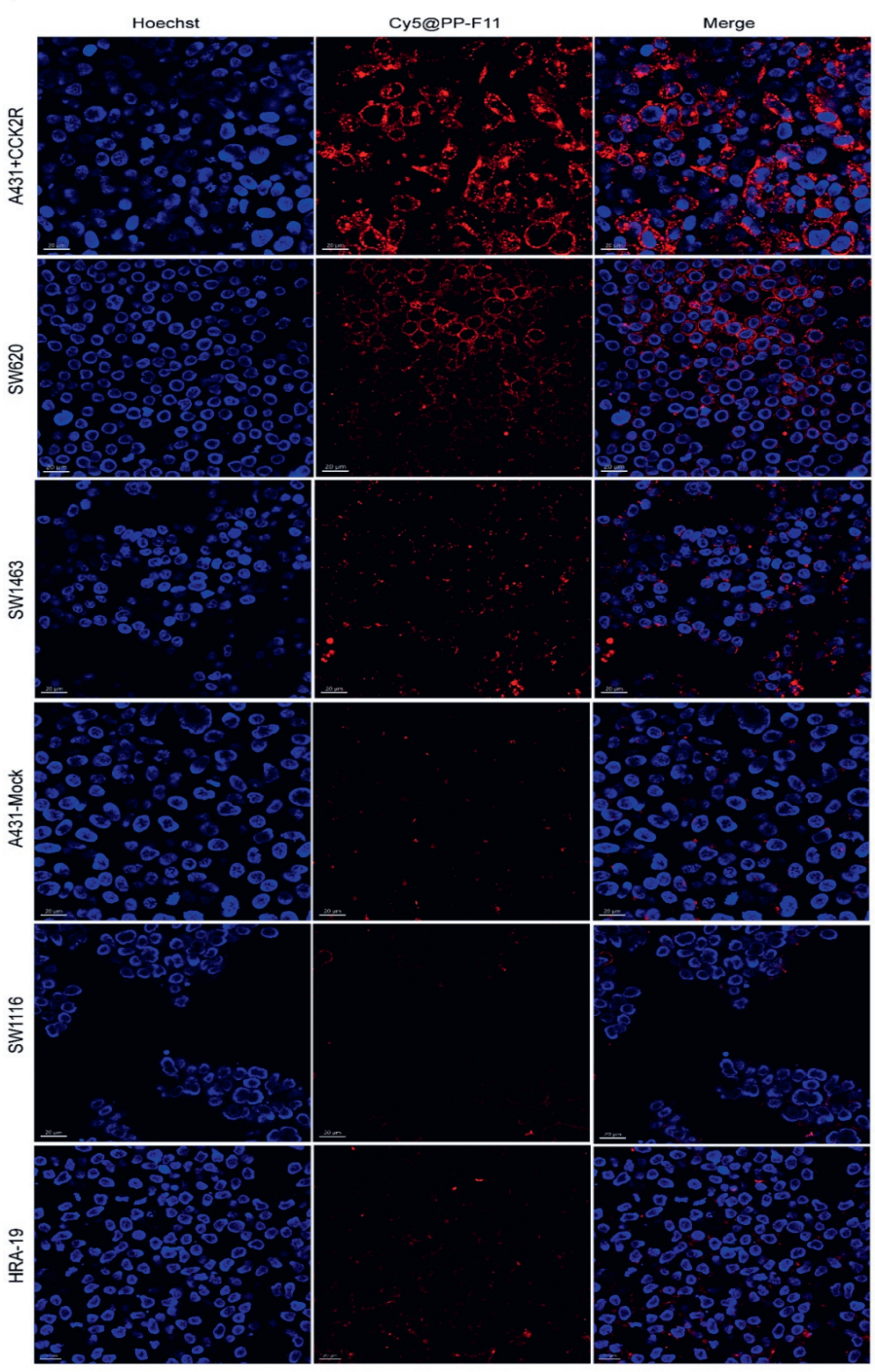
Hoechst
Cy5@PP-F11
Merge
A431+CCK2R
SW620
SW1463
A431-Mock
SW1116
HRA-19

Figure 2. Dragonfly 200 microscopy images showing Cy5@PP-F11 peptide binding in CCK2R-positive and negative cell lines. A431-CCK2R, SW620, SW1463, A431-Mock, SW1116, and HRA-19 cells were incubated with Cy5@PP-F11 peptide. Hoechst staining (blue) marks nuclei, and Cy5 fluorescence (red) indicates peptide binding. Strong fluorescence in A431-CCK2R and SW620 cells reflects high CCK2R expression, while moderate fluorescence in SW1463 suggests intermediate expression. In contrast, minimal fluorescence in A431-Mock, SW1116, and HRA-19 cells indicates low nonspecific binding due to negligible CCK2R expression. Scale bar = 20 µm.

Patient characteristics

From the initial TME trial cohort of 496 surgery only patients, individuals above 80 years (n=30) were excluded. Additional exclusions were applied based on TNM staging (M1: n=24) and WHO cancer type classifications, adenosquamous (n=1) and undifferentiated (n=1) carcinomas. Furthermore, patients with missing CCK2R values (n=76) and those with only one evaluable tissue punch (n=136) were excluded. The final dataset included 229 patients, with demographics and clinicopathological data summarized in (Table 1). Key variables assessed include epithelium percentage and its grouping, epithelium intensity and its grouping, overall epithelium and epithelium percentage* epithelium intensity (epithelium category), as well as stroma percentage and its grouping, stroma intensity and its grouping, overall stroma, and stroma percentage * stroma intensity (stroma category).

Table 1. **Baseline clinicopathological characteristics of rectal cancer patients (n = 229).** Data are presented as number of patients (*n*) and percentage (%) of the total cohort.

	Total (N=229)
Gender	
male	156 (68.1%)
female	73 (31.9%)
Age	
18-60	75 (32.8%)
60-80	154 (67.2%)
pTNM	
I	76 (33.2%)
II	60 (26.2%)
III	93 (40.6%)
WHO classification	
Adenocarcinoma	216 (94.3%)
mucinous	13 (5.7%)
Tumor grade	
well	14 (6.1%)
moderate	173 (75.5%)
poor or undifferentiated	42 (18.3%)
Adjuvant therapy	
Yes*	26 (11.4%)
No	203 (88.6%)
Circumferential margin	
negative	195 (85.2%)
positive	34 (14.8%)
Tumor infiltration	
circumscript	151 (65.9%)
diffuse	78 (34.1%)
Lymphoid reaction	
none/few	189 (82.5%)
extensive	40 (17.5%)
Eosinophils	
none/few	163 (71.2%)
moderate	52 (22.7%)
extensive	14 (6.1%)
Fibroblast reaction	
none/few	120 (52.4%)
moderate	85 (37.1%)
extensive	24 (10.5%)

Correlation of CCK2R epithelial staining with clinicopathological parameters in rectal cancer

CCK2R has been implicated in human tumorigenesis, with its expression levels previously linked to clinicopathological parameters in colon cancer [9, 20]. It has been reported that CCK2R is a promising biomarker for colorectal cancer due to its specific and high expression in the epithelial cells of primary tumors, which distinctly separates cancerous tissues from adjacent normal tissues. Its strong epithelial staining, demonstrated through immunohistochemistry, highlights its potential for diagnostic workflows, including histological evaluation and targeted imaging. This epithelial-specific expression further supports its utility in detecting early tumorigenic changes within the adenoma-carcinoma sequence [21]. In this study, we investigated CCK2R expression in rectal cancer, in relation with the clinicopathological characteristics of the patients. Using IHC staining, the epithelial and stromal expression of CCK2R was analyzed in samples from 229 rectal cancer patients. For the epithelial analysis, three variables were used to evaluate CCK2R expression. The first variable, epithelial percentage, represented the percentage of the epithelial area stained by IHC for expression of CCK2R. The second variable, epithelial intensity, measured the intensity of CCK2R expression staining within the epithelial regions, graded on a predefined scale. The third variable, epithelial category, was calculated by multiplying epithelial percentage and epithelial intensity, providing a combined metric to comprehensively assess epithelial CCK2R expression. The correlation between epithelial percentage, epithelial intensity, and epithelial category of CCK2R expression with clinical parameters was analyzed. As described above in CCK2R scoring methodology, scoring involved determining the percentage of epithelial or stromal areas stained with the CCK2R antibody (0 –100%) and grading staining intensity on a four-point scale: 1 (negative), 2 (weak), 3 (moderate), and 4 (strong). Representative examples of the different staining categories are shown in (Figure 3). For analysis, variables were recoded into low and high categories to facilitate comparisons. The clinicopathological characteristics of patients stratified by high (N=111) and low (N=118) CCK2R epithelium percentage are summarized in (Table 2). The stratification was based on the median tumor-epithelium CCK2R expression percentage (mean of all tumor tissue punches), with a cutoff value of 12.67%. Patients with expression values ≤12.67% were classified as the low expression group, and those with values >12.67% as the high expression group. No significant differences were observed between the two groups regarding sex, age, TNM staging, tumor differentiation, or tumor infiltration pattern. Most tumors in both groups were moderately differentiated adenocarcinomas, with stage III being the most common TNM classification. Among the analyzed variables, circumferential margin status showed a significant difference between groups ($p = 0.04$), with a higher percentage of positive margins in the high CCK2R group (19.8%) compared to the low CCK2R group (10.2%) (Figure 4). Additionally, while not statistically significant, a trend was observed in the distribution of histological subtypes ($p = 0.06$), with mucinous tumors more frequently found in the low CCK2R group (8.5%) compared to the high CCK2R group (2.7%). Similarly, lymphoid reaction approached significance ($p = 0.06$), with extensive reactions more prevalent in the low CCK2R group (22.0%) than in the high CCK2R group (12.6%). Other tumor microenvironment factors, such as eosinophil infiltration and fibroblast reaction, did not show statistically significant differences between groups, though a slight trend toward more extensive eosinophil infiltration was noted in the low CCK2R group.

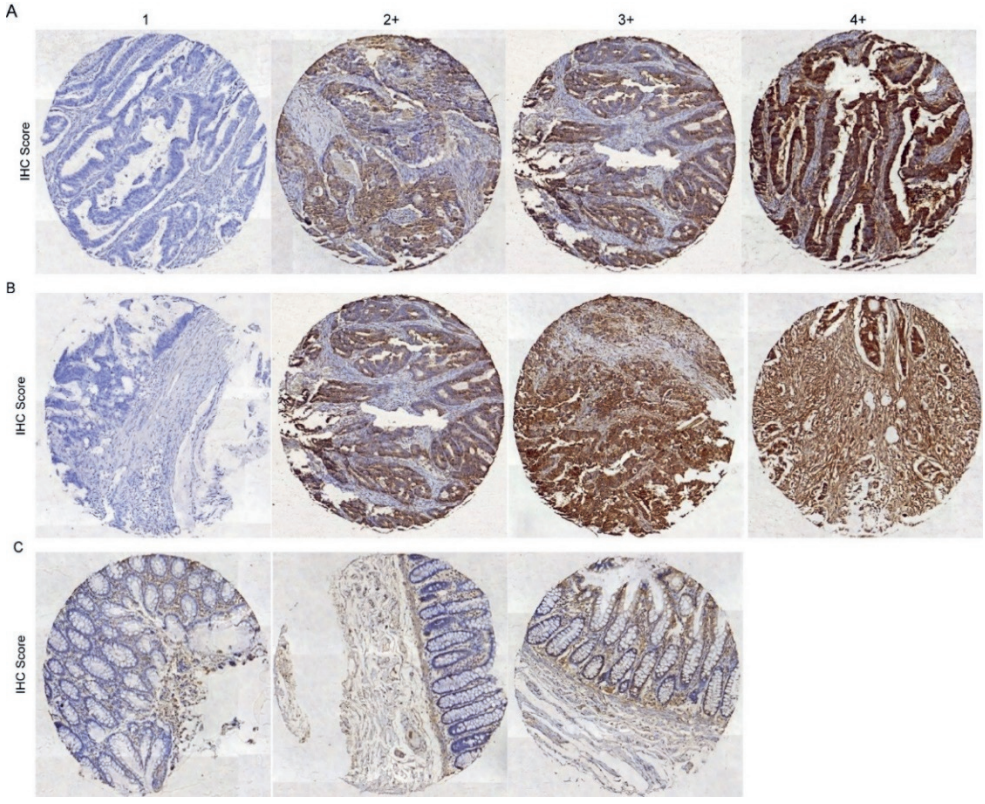

Figure 3. Expression levels of CCK2R in normal and rectal cancer tissues. (A) Representative IHC images illustrating epithelial CCK2R expression, scored as 1 (negative), 2+ (weak), 3+ (moderate), and 4+ (strong), along with the corresponding number and intensity of samples in each category. (B) Representative IHC images illustrating stromal CCK2R expression, assessed using the same scoring system. (C) Normal human rectal mucosa showing CCK2R expression, evaluated using the same IHC scoring criteria. None of the normal human rectal mucosa showed expression level 4+.

Table 2. Clinicopathological characteristics of rectal cancer patients stratified by epithelial CCK2R expression percentage. Data are presented as *n (%)*. Statistical comparisons were performed using the Chi-squared test. *P*-values < 0.05 were considered statistically significant and are marked with an asterisk (*).

	Low CCK2R epithelial percentage (N=118)	High CCK2R epithelial percentage (N=111)	Total (N=229)	P value
Gender				0.65
male	82 (69.5%)	74 (66.7%)	156 (68.1%)	
female	36 (30.5%)	37 (33.3%)	73 (31.9%)	
Age				0.51
<60	41 (34.7%)	34 (30.6%)	75 (32.8%)	
≥60	77 (65.3%)	77 (69.4%)	154 (67.2%)	
TNM				0.33
I	40 (33.9%)	36 (32.4%)	76 (33.2%)	
II	35 (29.7%)	25 (22.5%)	60 (26.2%)	
III	43 (36.4%)	50 (45.0%)	93 (40.6%)	
WHO classification				0.06
Adenocarcinoma	108 (91.5%)	108 (97.3%)	216 (94.3%)	
mucinous	10 (8.5%)	3 (2.7%)	13 (5.7%)	
Tumor grade				0.90
well	7 (5.9%)	7 (6.3%)	14 (6.1%)	
moderate	88 (74.6%)	85 (76.6%)	173 (75.5%)	
poor_undifferentiated	23 (19.5%)	19 (17.1%)	42 (18.3%)	
Adjuvant therapy				0.16
Yes	10 (8.5%)	16 (14.4%)	26 (11.4%)	
No	108 (91.5%)	95 (85.6%)	203 (88.6%)	
Circumferential margin				**0.04***
negative	106 (89.8%)	89 (80.2%)	195 (85.2%)	
positive	12 (10.2%)	22 (19.8%)	34 (14.8%)	
Tumor infiltration				0.24
circumscript	82 (69.5%)	69 (62.2%)	151 (65.9%)	
diffuse	36 (30.5%)	42 (37.8%)	78 (34.1%)	
Lymphoid reaction				0.06
none/few	92 (78.0%)	97 (87.4%)	189 (82.5%)	
extensive	26 (22.0%)	14 (12.6%)	40 (17.5%)	
Eosinophils				0.29
none/few	83 (70.3%)	80 (72.1%)	163 (71.2%)	
moderate	25 (21.2%)	27 (24.3%)	52 (22.7%)	
extensive	10 (8.5%)	4 (3.6%)	14 (6.1%)	
Fibroblast reaction				0.85
none/few	64 (54.2%)	56 (50.5%)	120 (52.4%)	
moderate	42 (35.6%)	43 (38.7%)	85 (37.1%)	
extensive	12 (10.2%)	12 (10.8%)	24 (10.5%)	

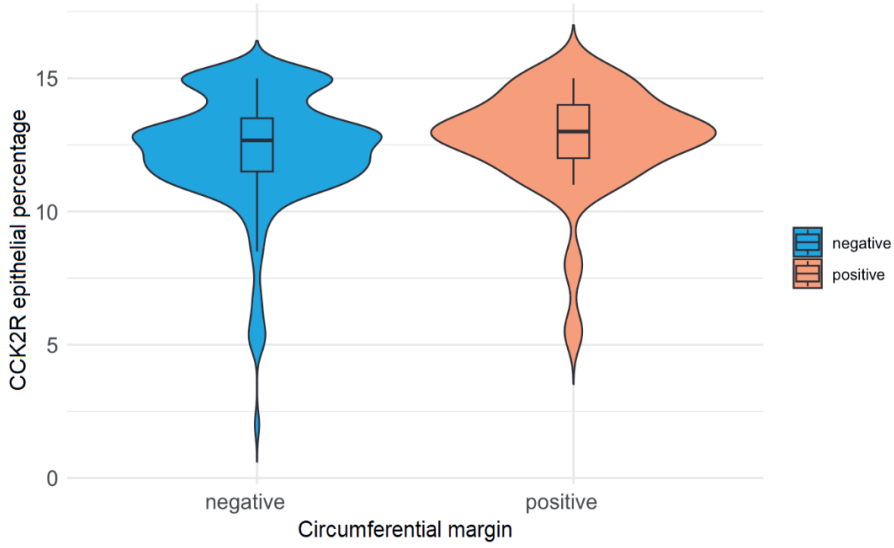

Figure 4. Violin plot showing the distribution of CCK2R expression epithelial percentage across circumferential margin categories (negative and positive). The width of each violin represents the kernel density estimation of the data distribution. Boxplots within the violins indicate the median, interquartile range (IQR), and potential outliers. The blue violin corresponds to the negative category, while the orange violin represents the positive category.

We analyzed the correlation between clinicopathological characteristics and the percentage of epithelial cells positive for CCK2R expression. No statistically significant differences were found between high (N=153) and low (N=76) intensity groups regarding sex, age, TNM staging, histological type, circumferential margin status, tumor infiltration pattern, lymphoid reaction, eosinophil infiltration, or fibroblast reaction. Tumor grade showed a trend in which moderately differentiated tumors were more frequent in the low-intensity group (82.9%) than in the high-intensity group (71.9%), while poorly/undifferentiated tumors were more common in the high group (20.9% vs. 13.2%) though this difference lacked statistical significance. Stage III remained the predominant TNM classification, and most tumors were adenocarcinomas. Similarly, no significant differences were observed based on epithelial category, which integrates intensity and percentage. Groups showed no notable variations in sex, age, TNM stage, histology, tumor differentiation, adjuvant therapy, or circumferential margin status. Tumor infiltration and lymphoid reaction showed trends, with circumscriptive infiltration and extensive lymphoid infiltration more frequent in the epithelium low group, while diffuse infiltration was prevalent in the epithelium high group (data not shown). CCK2R localization in cancer cells cytoplasmic, nuclear, or both offers valuable insights into its roles in tumor biology.

Cytoplasmic staining reflects its function as a G-protein-coupled receptor (GPCR) involved in intracellular signaling pathways regulating growth, migration, and survival. Nuclear staining suggests

roles in transcriptional regulation and chromatin interactions, potentially influencing tumor progression. Dual staining indicates complex regulatory mechanisms, linking CCK2R activity to both intracellular signaling and transcriptional functions. These patterns are associated with key clinicopathological outcomes, such as tumor differentiation, invasion, and prognosis [9, 20]. We also categorized staining localization for the epithelial regions as cytoplasmic, nuclear, or both and analyzed the clinicopathological characteristics of rectal cancer patients based on these patterns. The analysis revealed no significant differences between the cytoplasmic-only and dual (cytoplasmic and nuclear) (Supplementary Figure 2 A, B) staining groups. No cases exhibited nuclear-only staining (n = 0. TNM staging, histological type, tumor differentiation, adjuvant therapy status, circumferential margin involvement, tumor infiltration patterns, and immune response markers, including lymphoid reaction, eosinophil infiltration, and fibroblast reaction, all showed no significant differences, as all p-values were not significant (Supplementary Table 1).

Correlation of CCK2R stromal staining with clinicopathological parameters in rectal cancer

The expression of CCK2R in both stromal and epithelial compartments holds significant relevance in CRC biology. In epithelial cells, CCK2R is linked to tumorigenic signaling, including proliferation and migration. Stromal CCK2R expression reflects its role in the tumor microenvironment, where it may modulate fibroblast activity, immune cell infiltration, and extracellular matrix remodeling. Studies demonstrate that stromal cells often express higher levels of certain gastrointestinal peptide hormone receptors compared to epithelial cells, emphasizing the distinct yet complementary roles these compartments play in tumor progression [21]. The clinicopathological characteristics of rectal cancer patients, stratified by high (N=115) and low (N=114) stroma percentage of CCK2R expression, are detailed in (Table 3). Sex distribution, age, TNM staging, histological type, adjuvant therapy usage, circumferential margin status, tumor infiltration patterns, and immune response characteristics, including lymphoid reaction, eosinophil infiltration, and fibroblast reaction, showed no significant differences between groups. A significant association was observed in tumor differentiation ($p = 0.04$), with moderately differentiated tumors more common in the high stroma group, while poorly/undifferentiated tumors were more prevalent in the low stroma group (Figure 5).

Table 3. Clinicopathological characteristics of rectal cancer patients stratified by tumor stromal CCK2R expression percentage. Patients were grouped into low (<50%) and high (≥50%) stromal percentage categories. Data are presented as number (*n)* and percentage *(%)*. Statistical comparisons were performed using the Chi-squared test. *P*-values < 0.05 were considered statistically significant and are marked with an asterisk (*).

	Low CCK2R stroma percentage (N=114)	High CCK2R stroma percentage (N=115)	Total (N=229)	P value
Gender				0.92
male	78 (68.4%)	78 (67.8%)	156 (68.1%)	
female	36 (31.6%)	37 (32.2%)	73 (31.9%)	
Age				0.71
<60	36 (31.6%)	39 (33.9%)	75 (32.8%)	
≥60	78 (68.4%)	76 (66.1%)	154 (67.2%)	
TNM				0.64
I	36 (31.6%)	40 (34.8%)	76 (33.2%)	
II	33 (28.9%)	27 (23.5%)	60 (26.2%)	
III	45 (39.5%)	48 (41.7%)	93 (40.6%)	
WHO classification				0.76
Adenocarcinoma	107 (93.9%)	109 (94.8%)	216 (94.3%)	
mucinous	7 (6.1%)	6 (5.2%)	13 (5.7%)	
Tumor grade				**0.04***
well	8 (7.0%)	6 (5.2%)	14 (6.1%)	
moderate	78 (68.4%)	95 (82.6%)	173 (75.5%)	
poor_undifferentiated	28 (24.6%)	14 (12.2%)	42 (18.3%)	
Adjuvant therapy				0.66
Yes	14 (12.3%)	12 (10.4%)	26 (11.4%)	
No	100 (87.7%)	103 (89.6%)	203 (88.6%)	
Circumferential margin				0.69
negative	96 (84.2%)	99 (86.1%)	195 (85.2%)	
positive	18 (15.8%)	16 (13.9%)	34 (14.8%)	
Tumor infiltration				0.55
circumscript	73 (64.0%)	78 (67.8%)	151 (65.9%)	
diffuse	41 (36.0%)	37 (32.2%)	78 (34.1%)	
Lymphoid reaction				0.51
none/few	96 (84.2%)	93 (80.9%)	189 (82.5%)	
extensive	18 (15.8%)	22 (19.1%)	40 (17.5%)	
Eosinophils				0.81
none/few	83 (72.8%)	80 (69.6%)	163 (71.2%)	
moderate	25 (21.9%)	27 (23.5%)	52 (22.7%)	
extensive	6 (5.3%)	8 (7.0%)	14 (6.1%)	
Fibroblast reaction				0.78
none/few	61 (53.5%)	59 (51.3%)	120 (52.4%)	
moderate	40 (35.1%)	45 (39.1%)	85 (37.1%)	
extensive	13 (11.4%)	11 (9.6%)	24 (10.5%)	

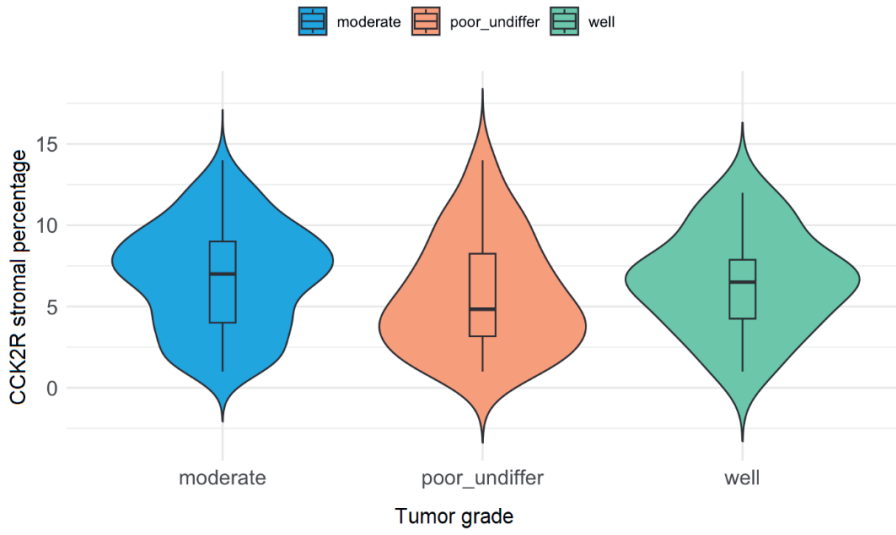

Figure 5. Violin plot of stroma percentage across tumor grade categories. This plot shows the distribution of stroma percentage (CCK2R expression) across tumor differentiation groups: moderate (blue), poorly/undifferentiated (orange), and well-differentiated (green). The violins represent data density, while box plots indicate the median and interquartile range. Stroma percentage varies across differentiation groups, with greater variability observed in poorly/undifferentiated tumors, highlighting its potential association with tumor differentiation.

The stromal compartment was scored by intensity, similar to the epithelial compartment, and its association with clinicopathological characteristics in rectal cancer was analyzed. Patients were classified into high (N=117) and low (N=112) stroma intensity groups based on CCK2R expression. No significant differences were observed between groups in sex distribution, age, TNM staging, histological type, adjuvant therapy use, circumferential margin status, or tumor infiltration patterns (data not shown). Tumor differentiation showed a notable trend, with moderately differentiated tumors more common in the high stroma group, while poorly/undifferentiated tumors were more frequent in the low stroma group. Lymphoid reaction showed a statistically significant difference ($p = 0.05$), with extensive lymphoid infiltration more common in the high stroma group (22.2%) than in the low stroma group (12.5%), suggesting a stronger immune response in tumors with high stroma intensity. It has been reported that CCK2R plays a crucial role in immune modulation by regulating CD4+ T cell differentiation. CCK-8 signaling through CCK2R suppresses pro-inflammatory Th1 and Th17 cells while enhancing regulatory T cells (Tregs), promoting an anti-inflammatory immune response. These findings suggest that CCK2R may influence lymphoid reactions by modulating immune cell infiltration and the balance of immune responses in the tumor microenvironment [22]. In addition, studies have shown that CCK2R modulates B cell function by suppressing differentiation and antibody production, thereby influencing immune responses. Given that extensive lymphoid infiltration was more common in the CCK2R-high stroma group, it is possible that stromal CCK2R plays a role in

shaping the tumor immune microenvironment, potentially affecting lymphoid aggregation and immune cell recruitment [23, 24]. Other tumor microenvironment characteristics, such as eosinophil infiltration (p = 0.78) and fibroblast reaction (p = 0.30), did not show significant differences between groups, though fibroblast reaction exhibited a slight trend, with extensive fibroblast reaction more common in the low stroma group (13.4% vs. 7.7%). These findings indicate that CCK2R stroma intensity may be associated with tumor differentiation and immune response, particularly in relation to lymphoid infiltration.

Table 4. Clinicopathological characteristics of rectal cancer patients stratified by stromal CCK2R expression category (stromal percentage × intensity). Patients were categorized into low (N = 82) and high (N = 147) stromal expression groups. Data are presented as number (*n)* and percentage *(%)*. Statistical comparisons were performed using the Chi-squared test. *P*-values < 0.05 were considered statistically significant and are marked with an asterisk (*).

	CCK2R-low stroma (N=82)	**CCK2R-high stroma (N=147)**	**Total (N=229)**	**P value**
				0.97
Gender				
male	56 (68.3%)	100 (68.0%)	156 (68.1%)	
female	26 (31.7%)	47 (32.0%)	73 (31.9%)	
Age				0.97
<60	27 (32.9%)	48 (32.7%)	75 (32.8%)	
≥60	55 (67.1%)	99 (67.3%)	154 (67.2%)	
TNM				**0.049***
I	26 (31.7%)	50 (34.0%)	76 (33.2%)	
II	29 (35.4%)	31 (21.1%)	60 (26.2%)	
III	27 (32.9%)	66 (44.9%)	93 (40.6%)	
WHO classification				0.84
Adenocarcinoma	77 (93.9%)	139 (94.6%)	216 (94.3%)	
mucinous	5 (6.1%)	8 (5.4%)	13 (5.7%)	
Tumor grade				0.06
well	8 (9.8%)	6 (4.1%)	14 (6.1%)	
moderate	55 (67.1%)	118 (80.3%)	173 (75.5%)	
poor_undifferentiated	19 (23.2%)	23 (15.6%)	42 (18.3%)	
Adjuvant therapy				0.76
Yes	10 (12.2%)	16 (10.9%)	26 (11.4%)	
No	72 (87.8%)	131 (89.1%)	203 (88.6%)	
Circumferential margin				0.95
negative	70 (85.4%)	125 (85.0%)	195 (85.2%)	
positive	12 (14.6%)	22 (15.0%)	34 (14.8%)	
Tumor infiltration				0.98
circumscript	54 (65.9%)	97 (66.0%)	151 (65.9%)	
diffuse	28 (34.1%)	50 (34.0%)	78 (34.1%)	
Lymphoid reaction				0.40
none/few	70 (85.4%)	119 (81.0%)	189 (82.5%)	

extensive	12 (14.6%)	28 (19.0%)	40 (17.5%)	
Eosinophils				0.40
none/few	62 (75.6%)	101 (68.7%)	163 (71.2%)	
moderate	17 (20.7%)	35 (23.8%)	52 (22.7%)	
extensive	3 (3.7%)	11 (7.5%)	14 (6.1%)	
Fibroblast reaction				0.22
none/few	37 (45.1%)	83 (56.5%)	120 (52.4%)	
moderate	34 (41.5%)	51 (34.7%)	85 (37.1%)	
extensive	11 (13.4%)	13 (8.8%)	24 (10.5%)	

Next, for the stromal compartment, we combined stromal percentage and stromal intensity to create a new variable, stromal category, which was analyzed for clinicopathological associations, as detailed in (Table 4). Patients were categorized into stromal low (N=82) and stromal high (N=147) groups based on CCK2R expression. Sex distribution, age, histological subtype, adjuvant therapy status, circumferential margin status, and tumor infiltration patterns showed no significant differences between group. TNM staging showed a significant association with stromal classification ($p = 0.049$), with stage III tumors more frequent in the stromal high group (44.9%) compared to the stromal low group (32.9%), whereas stage II tumors were more common in the stromal low group (35.4% vs. 21.1%) (Figure 6). BP Huang et al. reported that CCK2R was significantly associated with TNM staging in colon cancer, with higher cytoplasmic expression correlating with deeper tumor invasion (T stage, $p = 0.001$), venous invasion ($p = 0.023$), and advanced overall TNM stage ($p = 0.013$). However, these findings were based on CCK2R expression in the epithelial compartment, while its role in the stromal component remains unexplored [9, 24].

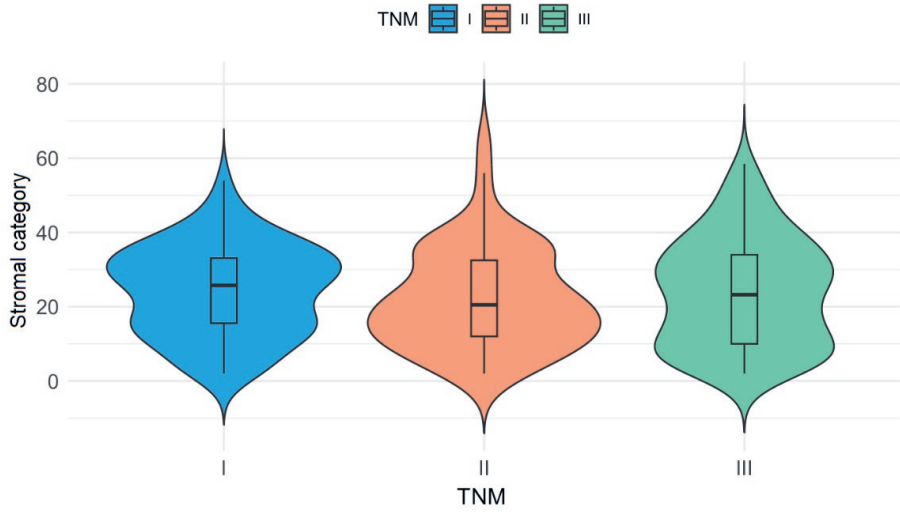

Figure 6. Violin plot of stroma percentage across TNM categories. This plot shows the distribution of stromal category (stromal percentage * intensity) based on CCK2R expression across TNM stages: stage I (blue), stage II (orange), and stage III (green). Violin plots represent data density, while box plots indicate the median and interquartile range. Stroma percentage varies across stages, with a broader distribution in stage II tumors, suggesting potential differences in the tumor microenvironment across disease progression.

Expression of CCK2R in normal and cancer tissues

In this study, we analyzed CCK2R expression in 229 rectal cancer tissues and 107 normal rectal tissues using a non-paired comparison. CCK2R levels were assessed in both the epithelial and stromal compartments. A two-way ANOVA was used to evaluate the effects of tissue type (normal vs. tumor) and compartment (epithelium vs. stroma) on expression levels. The analysis revealed that CCK2R expression was significantly elevated in rectal cancer tissues compared to normal tissues (*Column Factor:* $F(2, 334) = 145.9$, $p < 0.0001$), accounting for 28.12% of the total variation. Additionally, there was a significant difference in expression between compartments (*Row Factor:* $F(228, 334) = 1.415$, $p = 0.0019$), explaining 31.11% of the variation. Epithelial CCK2R expression was significantly higher than stromal expression ($p < 0.01$), and both were elevated compared to normal tissue levels. These findings indicate that CCK2R is upregulated in rectal cancer, with distinct compartmental expression (Figure 7).

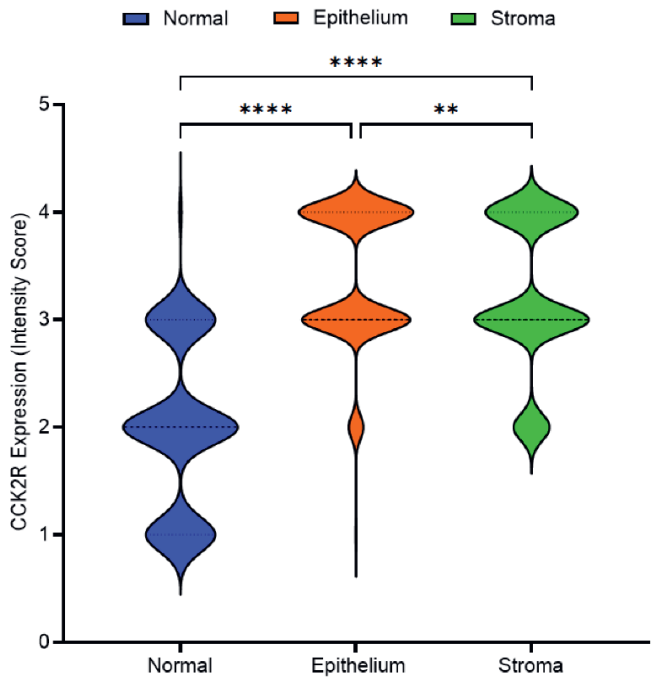

Figure 7. CCK2R expression in normal epithelium, cancer epithelium, and cancer-associated stroma. Violin plots show CCK2R expression intensity scores across normal epithelium (blue), cancerous epithelium (orange), and stroma (green). Black dashed lines represent the median and interquartile range. Two-way ANOVA revealed significantly higher CCK2R expression in both cancer epithelium and stroma compared to normal epithelium (***$p < 0.0001$), with cancer epithelium also significantly higher than stroma (*$p < 0.01$). Detailed statistical results are reported in the Results section.

CCK2R expression is associated with survival outcomes in rectal cancer

Given the relationship between CCK2R expression and clinical outcomes in RC, Kaplan–Meier (K–M) curves were utilized to assess overall survival (OS), disease-free survival (DFS), and distant recurrence-free survival (DRFS), as shown in (Figure 8, Figure 9, and Figure 10), respectively. Figure 9 presents Kaplan–Meier (K–M) survival curves for overall survival (OS) stratified by CCK2R epithelial expression and stromal characteristics. No significant differences in OS were observed when stratified by CCK2R epithelial percentage (Figure 8A, p = 0.21), CCK2R epithelial intensity (Figure 8C, p = 0.22), stroma intensity (Figure 8D, p = 0.12), or epithelial classification (Figure 8E, p = 0.14). In contrast, OS was significantly improved in cases with a higher stroma percentage (Figure 8B, p = 0.0075) and overall stromal classification (Figure 8F, p = 0.046). These findings suggest that stromal characteristics may have a greater impact on prognosis than CCK2R expression. DFS analysis in (Figure 9) shows Kaplan-Meier survival curves stratified by CCK2R expression in epithelial and stromal compartments. No significant differences in DFS were observed for CCK2R epithelial percentage (Figure 9A, p = 0.13), epithelial intensity (Figure 9C, p = 0.13), or epithelial classification (Figure 9E, p = 0.08). Similarly,

stroma intensity (Figure 9D, p = 0.13) did not show a significant association with DFS. However, a higher stroma percentage (Figure 9B, p = 0.02) was significantly linked to improved DFS, while stromal classification (Figure 9F, p = 0.052) showed a trend toward significance. These findings suggest that while CCK2R expression in the epithelial compartment does not strongly influence DFS, stromal characteristics particularly a higher stroma percentage play a more significant role in disease outcomes.

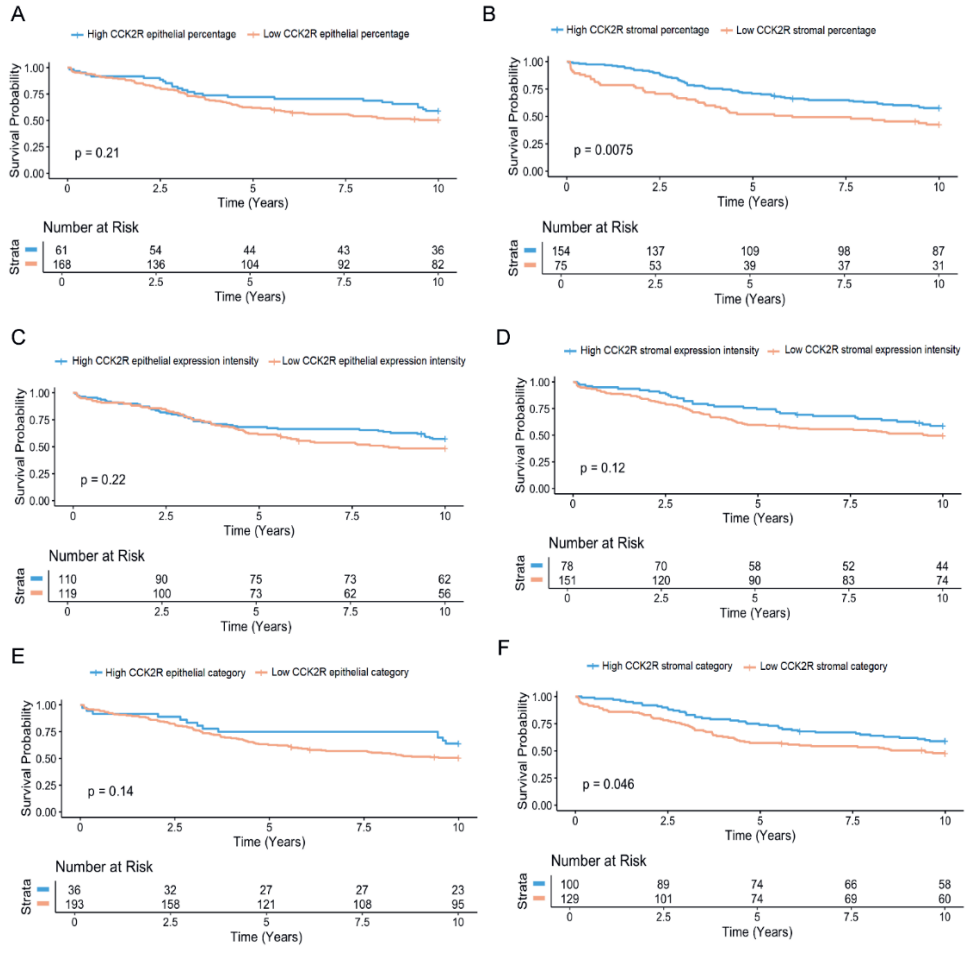

Figure 8. Kaplan-Meier survival curves comparing high and low CCK2R expression in epithelial and stromal compartments for Overall Survival (OS). Epithelium: No significant differences in OS were observed for CCK2R epithelial percentage (Figure 8A, p = 0.21), intensity (Figure 8C, p = 0.22), or epithelial category (Figure 8E, p = 0.14). Stroma: OS was not significantly affected by stroma intensity (Figure 8D, p = 0.12), but higher stroma percentage (Figure 8B, p = 0.0075) and overall stromal category (Figure 8F, p = 0.046) were associated with significantly improved OS.

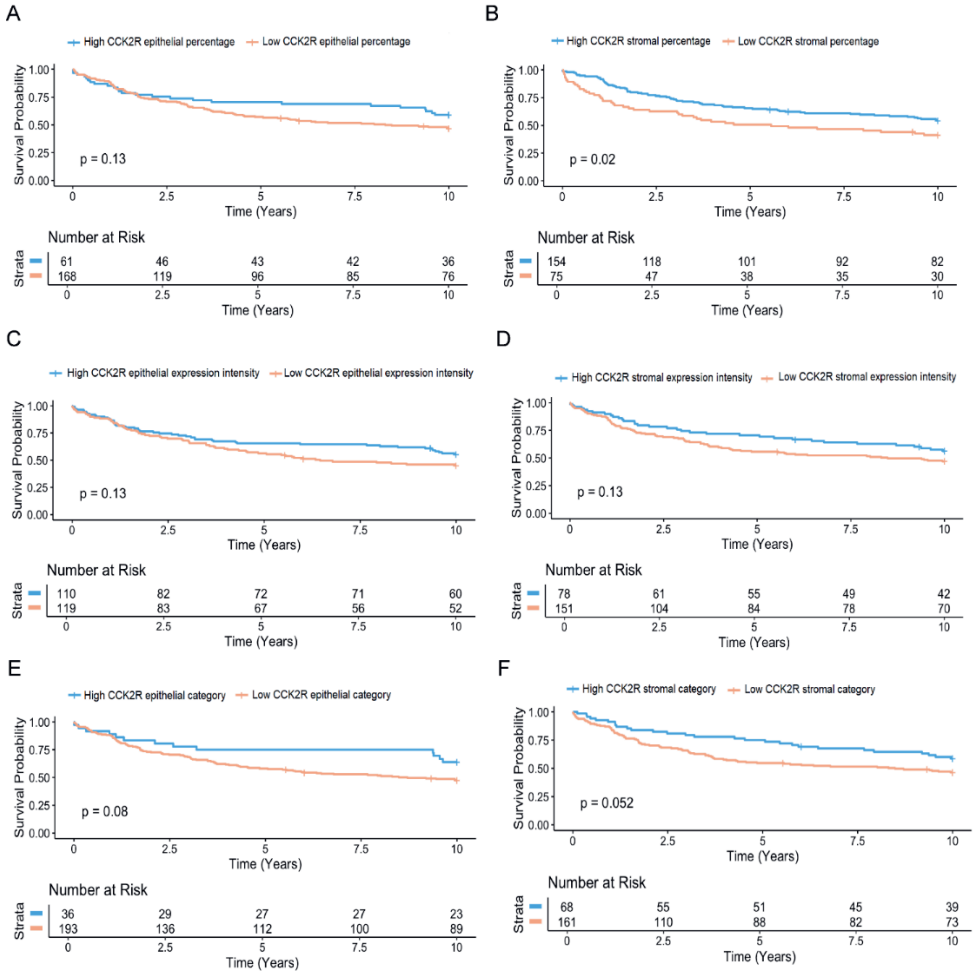

Figure 9. Kaplan-Meier survival curves for high and low CCK2R intensity in epithelial and stromal compartments across disease-free survival (DFS). Epithelium: No significant differences were observed for CCK2R epithelial percentage (Figure 9A, p = 0.13), intensity (Figure 9C, p = 0.13), or epithelial category (Figure 9E, p = 0.08). Stroma: DFS was not significantly affected by stroma intensity (Figure 9D, p = 0.13), but higher stroma percentage (Figure 9B, p = 0.02) was linked to improved DFS, with overall stromal category (Figure 9F, p = 0.052) showing a trend toward significance.

Finally, DRFS data in (Figure 10) highlighted the impact of CCK2R expression in epithelial and stromal compartments on distant recurrence-free survival. No significant differences were observed for CCK2R epithelial percentage (Figure 10A, p = 0.16), epithelial intensity (Figure 10C, p = 0.20), or stroma intensity (Figure 10D, p = 0.11). However, higher stroma percentage (Figure 10B, p = 0.031), epithelial category (Figure 10E, p = 0.021), and stroma category (Figure 10F, p = 0.021) were significantly associated with improved DRFS. These findings suggest that while CCK2R expression in the epithelium

does not have a strong prognostic impact, epithelial and stromal classifications particularly stromal features may play a more critical role in predicting distant recurrence-free survival.

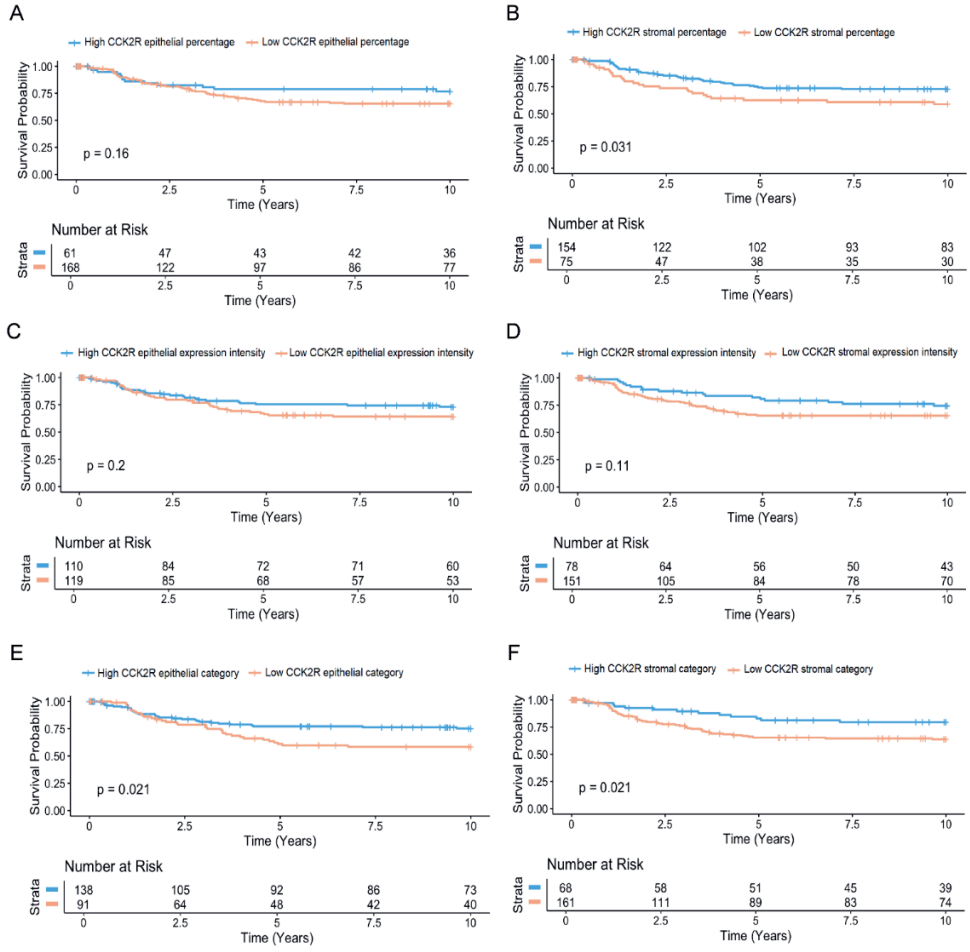

Figure 10. Kaplan-Meier survival curves for distant recurrence-free survival (DRFS) stratified by CCK2R expression in epithelial and stromal compartments. Epithelium: No significant differences were observed for CCK2R epithelial percentage (Figure 10A, p = 0.16) or intensity (Figure 10C, p = 0.20), while epithelial category (Figure 10E, p = 0.021) was significantly associated with improved DRFS. Stroma: Stroma intensity (Figure 10D, p = 0.11) showed no significant impact, but higher stroma percentage (Figure 10B, p = 0.031) and stroma category (Figure 10F, p = 0.021) were significantly linked to better DRFS.

Multivariable analysis

Univariate and multivariable analyses were performed to assess OS, DFS, and DRFS, as described above. The evaluated risk factors included circumferential margin, TNM stage, tumor grade, tumor

infiltration, lymphoid reaction, adjuvant therapy, CCK2R expression, and age. In the OS analysis, univariate Kaplan-Meier (KM) analysis identified stroma percentage (p = 0.0075) and stroma category (p = 0.046) as significant factors. However, multivariate cox regression analysis revealed no significant risk factors (data not shown), except for TNM stage III (p = 0.008). For DFS, univariate KM analysis showed that stroma percentage was the only significant factor (p = 0.02). In the multivariate cox regression analysis (Table 5), TNM stage III emerged as a significant independent prognostic factor for DFS (HR = 2.06, 95% CI 1.54–2.75, p = 0.007), while low stroma percentage remained significant (HR = 1.88, 95% CI 1.40–2.53, p = 0.04). Other factors, including gender, circumferential margin, tumor grade, tumor infiltration, lymphoid reaction, and adjuvant therapy, showed no significant associations with DFS.

Table 5. Multivariable Cox regression analysis of disease-free survival (DFS) in rectal cancer patients. Hazard ratios (HRs) and 95% confidence intervals (CIs) are presented. Statistical significance was set at $p < 0.05$.

	HR	Lower 95% CI	Upper 95% CI	P value
Gender				
<60	1			
≥60	1.13	0.75	1.69	0.57
Stromapercentage				
High	1			
Low	1.49	1.02	2.19	**0.04***
Circumferential margin				
negative	1			
positive	1.34	0.78	2.29	0.29
TNM				
I	1			
II	1.41	0.82	2.43	0.21
III	2.03	1.22	3.41	**0.007***
Tumor grade				
moderate	1			
poor_undifferentiated	1.12	0.69	1.80	0.65
well	1.07	0.49	2.35	0.87
Tumor infiltration				
circumscript	1			
diffuse	1.26	0.84	1.90	0.26
Lymphoid reaction				
none/few	1			
extensive	1.10	0.68	1.78	0.70
Adjuvant therapy				
Yes	1			
No	0.76	0.41	1.39	0.37

As previously reported, DRFS analysis results showed that in the univariate analysis, stroma percentage and combined stroma category (stroma percentage * intensity) were the only significant

factors in the Kaplan-Meier survival analysis. Multivariate cox regression analysis identified TNM stage II (HR = 1.97, 95% CI 1.05–3.69, p = 0.03) and poorly undifferentiated tumor grade (HR = 3.86, 95% CI 1.77–8.42, p = 0.0007) as significant independent prognostic factors for DRFS. Other factors, including gender, circumferential margin, tumor infiltration, lymphoid reaction, and adjuvant therapy, did not show significant associations with DRFS. These findings emphasize the prognostic significance of stroma characteristics, TNM stage II, and tumor grade in determining disease recurrence-free survival outcomes.

Table 6. Multivariable analysis of distant recurrence-free survival (DRFS) using Cox regression. Hazard ratios (HR), 95% confidence intervals (CI), and p-values are shown for each variable. Significant associations ($p < 0.05$) are indicated.

	HR	**Lower 95% CI**	**Upper 95% CI**	**P value**
Gender				
<60	1			
≥60	0.83	0.50	1.38	0.47
Stromapercentage				
High	1			
Low	1.34	0.77	2.34	0.29
Circumferential margin				
negative	1			
positive	1.87	0.94	3.74	0.08
TNM				
I	1			
II	1.97	1.05	3.69	**0.03***
III				
Tumor grade	1			
moderate	1.61	0.67	3.87	0.28
poor_undifferentiated	3.86	1.77	8.42	**0.0007***
well				
Tumor infiltration	1			
circumscript	1.06	0.57	1.96	0.85
diffuse	2.29	0.94	5.54	0.07
Lymphoid reaction				
none/few	1			
extensive	1.24	0.72	2.13	0.46
Adjuvant therapy				
Yes	1			
No	0.69	0.31	1.54	0.36

Discussion

The CCK2R has been a focal point in molecular imaging and targeted radionuclide therapy research for over two decades [25]. However, only a few studies have developed approaches to combine NIR dyes with CCK2R-targeting peptides for imaging of CCK2R-positive cancers [10, 26-28]. Two prior studies have documented the use of CCK2R-targeted NIR dyes for imaging superficial subcutaneous tumors, both utilizing minigastrin peptides derived from the sequence of endogenous gastrin as the targeting ligand [26, 27]. In another study, a nonpeptidic small molecule antagonist was utilized to target CCK2R and its splice variants for intraoperative imaging [10]. All three studies face limited tumor models and shallow imaging depth (~1 cm), restricting application to surface-accessible tumors. Kidney retention was a major issue, potentially affecting clinical use, while non-specific uptake in the GI tract reduced tumor contrast.

In the present study, we developed a NIR probe, Cy5@PP-F11, targeting CCK2R-positive cancer cells, utilizing the NIR fluorescent dye Cy5 for imaging applications. Specifically, we employed Cy5@PP-F11 to target CCK2R-positive cells, particularly in CRC and RC, building on previous studies that demonstrated the PP-F11 peptide's effective internalization of CCK2R-targeting agents in CCK2R-positive cancer cells. PP-F11 has emerged as a significant advancement in CCK2R-targeting radiopharmaceuticals, with strong potential for both imaging and treatment of CCK2R-expressing tumors [29-32]. In this study, we introduced specific modifications to PP-F11, including the addition of a Cy5 near-infrared fluorescent dye for imaging and $(GABOB)_2$-β-Ala spacers. The modified peptide was then utilized to achieve our research objectives. Our Cy5@PP-F11 probe demonstrated a high binding affinity in the nanomolar range (50 nM), with strong specificity and receptor-mediated internalization to a cytoplasmic location in a transfected cell model (A431+CCK2R) and SW620 cells, but not in CCK2R-negative cells. Importantly, the receptor-binding capability of the peptide remained intact after coupling to the Cy5 dye. While these *in vitro* findings highlight the potential of Cy5@PP-F11 as a targeted imaging probe for CCK2R, we note that it's *in vivo* performance has not yet been evaluated, and thus its applicability for intraoperative imaging remains to be validated in future studies.

This research identified significant overexpression of CCK2R in both the stromal and epithelial compartments of RC TMA tissues, with expression levels notably elevated compared to normal rectal tissues. These findings mark a novel observation that extends beyond previous research, which primarily focused on the epithelial expression of CCK2R in colorectal cancer [8]. Furthermore, this study is the first to demonstrate a significant association between CCK2R expression and clinicopathological characteristics in RC. This dual localization highlights the potential for CCK2R to play a more intricate role within the tumor microenvironment of rectal cancer, influencing both tumor cells and their supportive stromal components. The data showed that CCK2R expression was significantly higher in both the epithelial and stromal compartments compared to normal rectal tissues, emphasizing its dual localization within the tumor microenvironment.

Previous studies on CCK2R in colorectal cancer have primarily focused on its overexpression in epithelial cells, where it drives tumor growth, proliferation, and survival through pathways such as PI3K/AKT and MAPK [8, 33]. Therapeutic strategies targeting epithelial CCK2R, including radiolabeled peptides and immunotoxins, have shown promising results, demonstrating the receptor's potential as

a therapeutic target [8]. We evaluated CCK2R overexpression in the epithelial compartment by assessing both the percentage of positive cells and the intensity of expression. Our findings demonstrate significant overexpression of CCK2R in the epithelial compartment of rectal cancer, consistent with its established tumor-promoting role in CRC. However, no significant correlation was observed between epithelial CCK2R overexpression and tumor stage or other clinicopathological characteristics in our cohort except circumferential margin ($p = 0.04$). As we discussed before, this aligns with previous a study where CCK2R expression was not always associated with traditional clinical parameters but was still implicated in tumor progression through its oncogenic signaling pathways [8]. The oncogenic role of CCK2R has been established in epithelial tumor cells, with mutations driving tumor growth, angiogenesis, and invasion [34]. However, the role of CCK2R in the stromal compartment remains less understood. Given that our study found an association between high stromal CCK2R expression and increased lymphoid infiltration ($p= 0.05$), it is possible that stromal CCK2R contributes to immune modulation within the tumor microenvironment. While previous studies [34] have demonstrated that CCK2R activation can promote pro-tumorigenic signaling, its stromal expression may have distinct immunoregulatory effects that warrant further investigation. While most studies on CCK2R have focused on its expression in the epithelial compartment, limited evidence exists regarding its role in the stromal compartment. One study identified the presence of functional gastrointestinal hormone receptors, including CCK2R, in the stromal cells of CRC, suggesting a potentially broader role for this receptor in the tumor microenvironment [21]. Our research addresses this gap by demonstrating significant CCK2R overexpression in both the epithelial and stromal compartments of rectal cancer, marking a novel observation. Our data showed a significant correlation between stromal CCK2R overexpression and tumor grade ($p = 0.04$) and TNM staging ($p = 0.049$). This dual localization underscores the potential role of CCK2R in tumor-stroma interactions, contributing to a more complex tumor microenvironment.

Multiple studies have shown significantly elevated CCK2R expression in CRC tissues compared to normal tissues, highlighting its role in tumor progression and potential as a biomarker and therapeutic target. CCK2R is primarily found in the epithelial regions of CRC, with minimal or absent expression in normal mucosa, and occasional weak expression in the muscular layers of normal tissues [11, 33]. One study demonstrated that 36.6% of CRC samples exhibited significant CCK2R expression using IHC, whereas adjacent normal tissues lacked detectable levels of the receptor. This selective overexpression underscores CCK2R's utility in distinguishing tumor tissues from normal counterparts [8]. Another report identified CCK2R mRNA expression in 38% of CRC samples, compared to 13% in normal tissues. Importantly, co-expression of CCK2R and its ligand gastrin was observed in 32% of CRC samples but not in normal mucosa, suggesting a functional autocrine loop that may promote tumorigenesis [35]. In conclusion, while normal tissues such as the pancreas, stomach, liver, and lung exhibit consistent but lower levels of CCK2R expression, its significant overexpression in rectal cancer tissues, as demonstrated in this study, highlights its potential role in tumor progression. In our study, CCK2R expression was significantly higher in rectal cancer tissues, with both epithelial and stromal compartments showing elevated levels compared to normal tissue.

CCK2R expression in both the epithelial and stromal compartments provides valuable insight into the behavior of rectal tumors and patient outcomes. OS showed no significant differences, a trend toward worse survival in the low stromal CCK2R category and high stromal CCK2R percentage suggests that

the tumor microenvironment, particularly the stroma, plays a crucial role in disease progression. DFS analysis links low stromal CCK2R expression to earlier recurrence, implying a role in tumor aggressiveness and therapy resistance. The J. Chang et al. study [8] linked high epithelial CCK2R expression to shorter DFS, suggesting its role in recurrence, while our study found no significant DFS association but a trend indicating lower epithelial CCK2R may predict poorer prognosis. This difference may stem from variations in cohorts, tumor subtypes, or scoring methods. Unlike the J. Chang et al. study [8], which analyzed only epithelial expression, our study provided a more detailed evaluation, incorporating both epithelial and stromal compartments.

These results suggest stromal CCK2R is crucial for tumor progression and prognosis, making it a potential biomarker in rectal cancer. CCK2R regulates T cell differentiation, suppresses Th1/Th17 responses, and enhances Tregs, creating an anti-inflammatory immune environment. It also affects B cell activity and antigen presentation. With higher lymphoid infiltration in the high stroma group, stromal CCK2R may influence immune recruitment and tumor regulation. Its deficiency impairs antigen presentation and immune balance, further supporting its role in the tumor microenvironment [22-24, 36]. Our DRFS findings further link low stromal CCK2R expression to increased metastasis risk, likely through angiogenesis or extracellular matrix remodeling. Targeting stromal CCK2R may offer a strategy to prevent tumor dissemination.

Conclusion

Our research highlights the significant overexpression of CCK2R in both the epithelial and stromal compartments of rectal cancer, with stromal CCK2R demonstrating a notable association with tumor-stroma interactions and the tumor microenvironment. Its correlation with tumor grade and TNM staging suggests a potential prognostic role in rectal cancer. Additionally, the development of Cy5@PP-F11 as a fluorescence probe for CCK2R-targeted imaging presents a promising strategy for enhancing intraoperative tumor visualization. These findings support the potential of stromal CCK2R as both a prognostic biomarker and a therapeutic target, warranting further investigation into its clinical applications.

Expression of Cholecystokinin 2 Receptor (CCK2R) in Rectal Cancer: Clinical Relevance and In Vitro Targeting with a Fluorescent CCK2R-Binding Peptide

Somayeh Rezaei, Xi Zhang, Ronald L.P. van Vlierberghe, Amber Piet, Elma Meershoek-Klein Kranenbarg, Ajinkya Manelkar, Yann Seimbille, Peter Laverman, Louise van der Weerd, Alexander L. Vahrmeijer, and Peter J.K. Kuppen. Z

Pharmacological Research Reports

Supplementary Materials

Peptides. The cholecystokinin 2 receptor (CCK2R) targeting peptide, PP-F11, was modified to enhance its functionality for imaging applications. The resulting peptide, Cy5-$(GABOB)_2$-β-Ala-Trp-(N-Me)Nle-Asp-1-Nal-NH_2 (Cy5@PP-F11), includes a Cyanine 5 (Cy5) near-infrared fluorescent dye for imaging and $(GABOB)_2$-β-Ala spacers to improve solubility, stability, and flexibility. These modifications build upon the core sequence of PP-F11, which is designed for high affinity binding to CCK2R, by adding features optimized for near-infrared fluorescence imaging.

Unless stated otherwise, all reagents and solvents were obtained commercially and used without further purification. Characterization by liquid chromatography-mass spectrometry (LC-MS) was carried out using an Agilent InfinityLab LC/MSD system equipped with an InfinityLab Poroshell 120 EC-C18 column (3 x 100 mm, 2.7 µm), measuring absorbance at 230, 254, and 280 nm. Samples were eluted from the column over 8 minutes using a bi-phasic system of 0.1% formic acid in H_2O (**A**) and 0.1% formic acid in acetonitrile (**B**), decreasing the polarity over time from 95:5 to 0:100 **A/B** (5 min). Purification by high-performance liquid chromatography (HPLC) was achieved using an Agilent 1260 Infinity II HPLC system (Middelburg, The Netherlands) equipped with an Agilent 5 Prep C18 column (50 x 21.2 mm) (Middelburg, The Netherlands). All peptides were provided by Yann Seimbille at Erasmus MC University, Netherlands.

To synthesize the $(GABOB)_2$-β-Ala-Trp-(N-Me)Nle-Asp-1-Nal-NH_2 sequence, standard Fmoc-based solid-phase peptide synthesis (SPPS) conditions were used. Conjugation to the rink amide 4-methylbenzhydrylamine (MBHA) resin (286 mg, average loading capacity: 0.65 mmol/g) was achieved by adding the corresponding amino acid (4 equiv.), hexafluorophosphate azabenzotriazole tetramethyl uronium (HATU; 4 equiv.), and diisopropylethylamine (DIPEA; 8 equiv.) in dimethylformamide (DMF), before gently agitating the reaction mixture at room temperature (rt) for 3 h. Fmoc deprotection was achieved using a 20% piperidine solution in DMF (2 x 15 min). Amide formation and Fmoc deprotection were monitored by Kaiser test. Amino acids were introduced to the resin in the following sequence: Fmoc-1-Nal-OH, Fmoc-*L*-Asp(OtBu)-OH, Fmoc-*N*-Me-Nle-OH, Fmoc-*L*-Trp(Boc)-OH, Fmoc-β-Ala-OH, Fmoc-GABOB-OH, Fmoc-GABOB-OH. Cleavage and removal of the Boc-protecting groups was achieved by treating the resin with a mixture of trifluoroacetic acid/water/thioanisole/1,2-ethanedithiol (TFA/H_2O/thioanisole/EDT, v/v/v/v = 84.5:8:5:2.5) for 3.5 h. The filtrate was collected and concentrated under airflow before precipitating in ice-cold diethyl

ether. The precipitate was purified by HPLC. A bi-phasic system of 0.1% TFA in H_2O (**A**) and 0.1% TFA in acetonitrile (**B**) was used to elute the product, decreasing the polarity of the solvent mixture over time in a gradient from 85:15 to 70:30 **A/B** (8 min), from 70:30 to 50:50 **A/B** (6 min), and from 50:50 to 0:100 **A/B** (2 min) at a flowrate of 10 mL/min. Following lyophilization, NH_2-(GABOB)$_2$-β-Ala-Trp-(N-Me)Nle-Asp-1-Nal-NH_2 was obtained as a white powder (28 mg, 0.03 mmol, 30% yield). LC: R_t = 4.281 min; purity: >99%; ESI-MS: *m/z*, calculated: 915.45, found: 916.50 $[M + H]^+$.

To NH_2-(GABOB)$_2$-β-Ala-Trp-(N-Me)Nle-Asp-1-Nal-NH_2 (10.4 mg, 0.01 mmol, 1 equiv.) was added a solution of Cy5 ester NHS (7.6 mg, 0.01 mmol, 1 equiv.) and DIPEA (30.4 µl, 0.18 mmol, 16 equiv.) in DMF (6 mL). The reaction mixture was left to stir at rt under dark conditions overnight, after which the mixture was concentrated *in vacuo* and purified by HPLC. A bi-phasic system of 0.1% TFA in H_2O (**A**) and 0.1% TFA in acetonitrile (**B**) was used to elute the product, decreasing the polarity of the solvent mixture over time in a gradient from 85:15 to 40:60 **A/B** (2 min), from 40:60 to 25:75 **A/B** (6 min), and from 25:75 to 0:100 **A/B** (2 min) at a flowrate of 10 mL/min. Cy5@PP-F11 was obtained as a dark-blue powder (9.2 mg, 0.007 mmol, 60.5% yield). LC: R_t = 5.341 min; purity: >97%; ESI-MS: *m/z*, calculated: 1380.74, found: 690.90 $[M + 2H]^{2+}$.

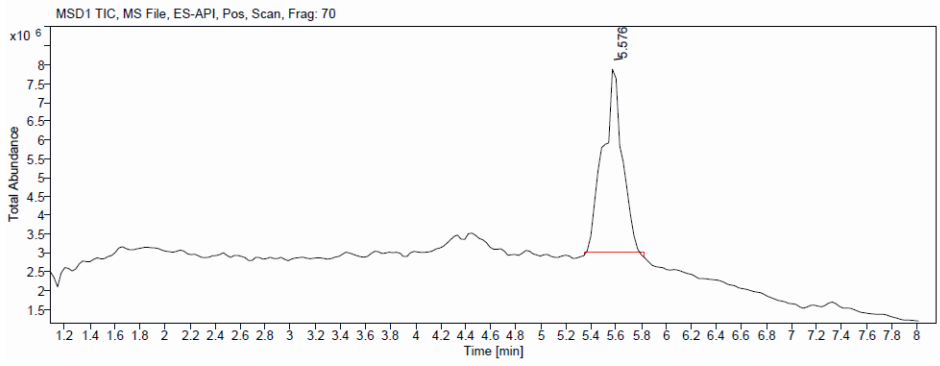

RT	Peak Width 5 Perc	Height	Peak Height Percent	Area	Rel. Area
[min]	[count]			[count*min]	[%]
5.576	0.400	5112701	100.00	52356100	100.0

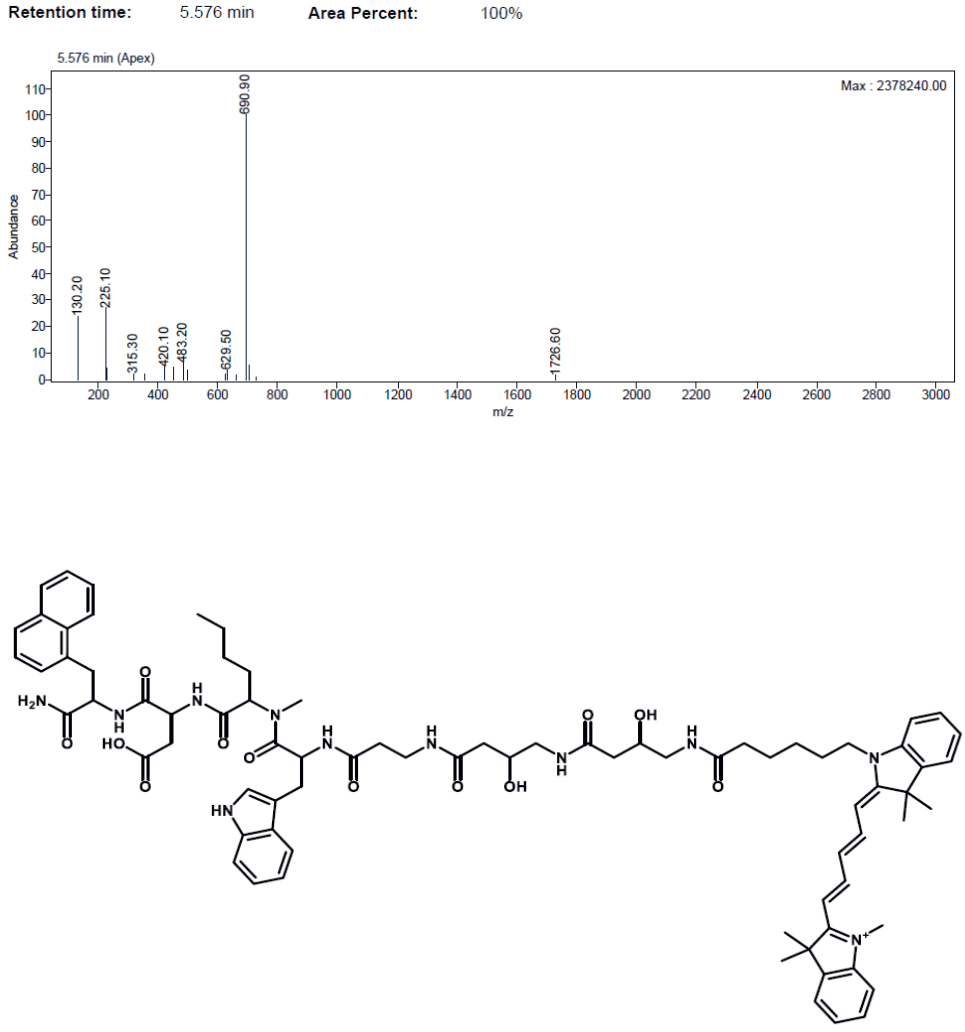

Supplementary Figure 1. Chemical structure of the Cy5@PP-F11 peptide (Cy5-$(GABOB)_2$-β-Ala-Trp-(N-Me)Nle-Asp-1-Nal-NH_2).

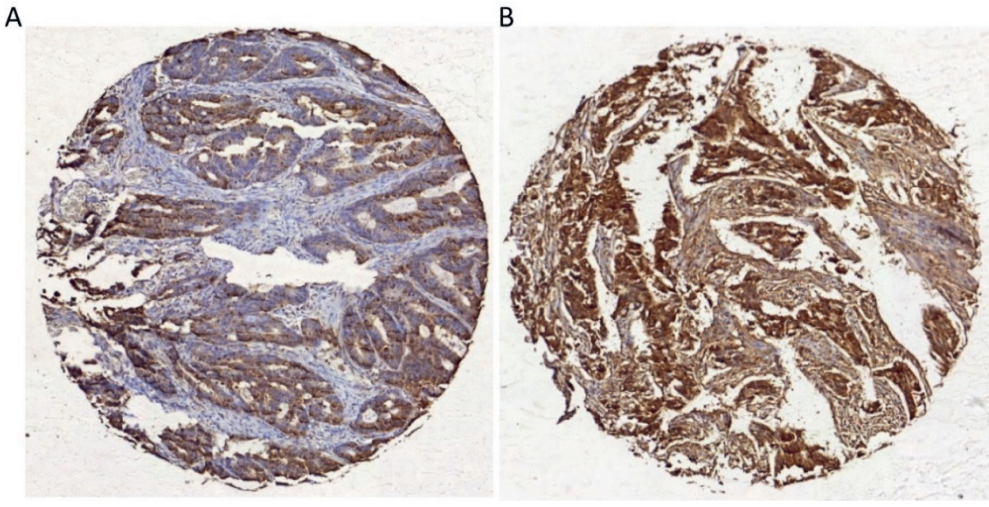

Supplementary Figure 2. Representative IHC images illustrating epithelial CCK2R expression. (A) Predominantly cytoplasmic staining. (B) Combined cytoplasmic and nuclear staining**.**

Supplementary Table 1. Clinicopathological characteristics of the patient cohort in relation with expression of CCK2R. Expression of CCK2R was determined by immunohistochemistry. There was no statistical significant correlation between CCK2R expression and any of the clinicopathological characteristics.

	Cytoplasmic CCK2R expression only (N=135)	Cytoplasmic and nuclear CCK2R expression (N=26)	Total (N=161)
Gender			
male	98 (72.6%)	21 (80.8%)	119 (73.9%)
female	37 (27.4%)	5 (19.2%)	42 (26.1%)
Age			
<60	47 (34.8%)	5 (19.2%)	52 (32.3%)
≥60	88 (65.2%)	21 (80.8%)	109 (67.7%)
TNM			
I	48 (35.6%)	6 (23.1%)	54 (33.5%)
II	31 (23.0%)	9 (34.6%)	40 (24.8%)
III	56 (41.5%)	11 (42.3%)	67 (41.6%)
WHO classification			
Adenocarcinoma	129 (95.6%)	23 (88.5%)	152 (94.4%)
mucinous	6 (4.4%)	3 (11.5%)	9 (5.6%)
Tumor grade			
Well	9 (6.7%)	1 (3.8%)	10 (6.2%)
moderate	101 (74.8%)	21 (80.8%)	122 (75.8%)
poor_undiffer	25 (18.5%)	4 (15.4%)	29 (18.0%)
Adjuvant therapy			
Yes	15 (11.1%)	4 (15.4%)	19 (11.8%)
No	120 (88.9%)	22 (84.6%)	142 (88.2%)
Circumferential margin			
negative	114 (84.4%)	19 (73.1%)	133 (82.6%)
positive	21 (15.6%)	7 (26.9%)	28 (17.4%)
Tumor infiltration			
circumscript	87 (64.4%)	17 (65.4%)	104 (64.6%)
diffuse	48 (35.6%)	9 (34.6%)	57 (35.4%)
Lymphoid reaction			
none/few	115 (85.2%)	21 (80.8%)	136 (84.5%)
extensive	20 (14.8%)	5 (19.2%)	25 (15.5%)
Eosinophils			
none/few	100 (74.1%)	16 (61.5%)	116 (72.0%)
moderate	27 (20.0%)	7 (26.9%)	34 (21.1%)
extensive	8 (5.9%)	3 (11.5%)	11 (6.8%)
Fibroblast reaction			
none/few	71 (52.6%)	12 (46.2%)	83 (51.6%)
moderate	50 (37.0%)	12 (46.2%)	62 (38.5%)
extensive	14 (10.4%)	2 (7.7%)	16 (9.9%)

References

[1] F. Bray, M. Laversanne, H. Sung, J. Ferlay, R.L. Siegel, I. Soerjomataram, A. Jemal, Global cancer statistics 2022: GLOBOCAN estimates of incidence and mortality worldwide for 36 cancers in 185 countries, CA: a cancer journal for clinicians 74(3) (2024) 229-263.
[2] A.M. Wolf, E.T. Fontham, T.R. Church, C.R. Flowers, C.E. Guerra, S.J. LaMonte, R. Etzioni, M.T. McKenna, K.C. Oeffinger, Y.C.T. Shih, Colorectal cancer screening for average‐risk adults: 2018 guideline update from the American Cancer Society, CA: a cancer journal for clinicians 68(4) (2018) 250-281.
[3] E.R. Fearon, B. Vogelstein, A genetic model for colorectal tumorigenesis, cell 61(5) (1990) 759-767.
[4] E.P. van der Stok, M.C. Spaander, D.J. Grünhagen, C. Verhoef, E.J. Kuipers, Surveillance after curative treatment for colorectal cancer, Nature reviews Clinical oncology 14(5) (2017) 297-315.
[5] B. Levin, D.A. Lieberman, B. McFarland, K.S. Andrews, D. Brooks, J. Bond, C. Dash, F.M. Giardiello, S. Glick, D. Johnson, Screening and surveillance for the early detection of colorectal cancer and adenomatous polyps, 2008: a joint guideline from the American Cancer Society, the US Multi-Society Task Force on Colorectal Cancer, and the American College of Radiology, Gastroenterology 134(5) (2008) 1570-1595.
[6] R. Glynne-Jones, L. Wyrwicz, E. Tiret, G. Brown, C.d. Rödel, A. Cervantes, D. Arnold, Rectal cancer: ESMO Clinical Practice Guidelines for diagnosis, treatment and follow-up, Annals of Oncology 28 (2017) iv22-iv40.
[7] J. Roy, K.S. Putt, D. Coppola, M.E. Leon, F.K. Khalil, B.A. Centeno, N. Clark, V.E. Stark, D.L. Morse, P.S. Low, Assessment of cholecystokinin 2 receptor (CCK2R) in neoplastic tissue, Oncotarget 7(12) (2016) 14605.
[8] J. Chang, Z.-S. Liu, D.-F. Song, M. Li, S. Zhang, K. Zhao, Y.-T. Guan, H.-L. Ren, Y.-S. Li, Y. Zhou, Cholecystokinin type 2 receptor in colorectal cancer: diagnostic and therapeutic target, Journal of Cancer Research and Clinical Oncology 146 (2020) 2205-2217.
[9] B.-P. Huang, C.-H. Lin, Y.-C. Chen, S.-H. Kao, Expression of cholecystokinin receptors in colon cancer and the clinical correlation in Taiwan, Tumor Biology 37 (2016) 4579-4584.
[10] C. Wayua, P.S. Low, Evaluation of a cholecystokinin 2 receptor-targeted near-infrared dye for fluorescence-guided surgery of cancer, Molecular pharmaceutics 11(2) (2014) 468-476.
[11] J. Chang, X. Liu, H. Ren, S. Lu, M. Li, S. Zhang, K. Zhao, H. Li, X. Zhou, L. Peng, Pseudomonas exotoxin A-based immunotherapy targeting CCK2R-expressing colorectal malignancies: an in vitro and in vivo evaluation, Molecular Pharmaceutics 18(6) (2021) 2285-2297.
[12] G. Jin, V. Ramanathan, M. Quante, G.H. Baik, X. Yang, S.S. Wang, S. Tu, S.A. Gordon, D.M. Pritchard, A. Varro, Inactivating cholecystokinin-2 receptor inhibits progastrin-dependent colonic crypt fission, proliferation, and colorectal cancer in mice, The Journal of clinical investigation 119(9) (2009) 2691-2701.
[13] C. Wang, Z. Wang, T. Zhao, Y. Li, G. Huang, B.D. Sumer, J. Gao, Optical molecular imaging for tumor detection and image-guided surgery, Biomaterials 157 (2018) 62-75.
[14] S.B. Mondal, S. Gao, N. Zhu, R. Liang, V. Gruev, S. Achilefu, Real-time fluorescence image-guided oncologic surgery, Advances in cancer research 124 (2014) 171-211.
[15] M.C. Boonstra, H.A. Prevoo, J. Kuil, M.W. Bordo, L.S. Boogerd, B.G.S. Mulder, C.F. Sier, M.L. Vinkenburg-van Slooten, A.R.P. Valentijn, J. Burggraaf, Real-time near-infrared fluorescence imaging using cRGD-ZW800-1 for intraoperative visualization of multiple cancer types, Oncotarget 8(13) (2017) 21054.

[16] A.A. Hörmann, M. Klingler, C. Rangger, C. Mair, L. Joosten, G.M. Franssen, P. Laverman, E. von Guggenberg, Effect of N-terminal peptide modifications on in vitro and in vivo properties of 177Lu-labeled peptide analogs targeting CCK2R, Pharmaceutics 15(3) (2023) 796.
[17] M. Klingler, D. Summer, C. Rangger, R. Haubner, J. Foster, J. Sosabowski, C. Decristoforo, I. Virgolini, E. von Guggenberg, DOTA-MGS5, a new cholecystokinin-2 receptor-targeting peptide analog with an optimized targeting profile for theranostic use, Journal of Nuclear Medicine 60(7) (2019) 1010-1016.
[18] A.W. Sauter, R. Mansi, U. Hassiepen, L. Muller, T. Panigada, S. Wiehr, A.-M. Wild, S. Geistlich, M. Béhé, C. Rottenburger, Targeting of the cholecystokinin-2 receptor with the minigastrin analog 177Lu-DOTA-PP-F11N: does the use of protease inhibitors further improve in vivo distribution?, Journal of Nuclear Medicine 60(3) (2019) 393-399.
[19] M.S. Reimers, C.C. Engels, H. Putter, H. Morreau, G.J. Liefers, C.J. van de Velde, P.J. Kuppen, Prognostic value of HLA class I, HLA-E, HLA-G and Tregs in rectal cancer: a retrospective cohort study, BMC cancer 14 (2014) 1-12.
[20] B.-P. Huang, C.-H. Lin, S.-H. Kao, Cholecystokinin Type A Receptor Expression Is Correlated with Poor Survival in Patients with Colon Cancer, Tungs' Medical Journal.
[21] C. Chao, M.L. Tallman, K.L. Ives, C.M. Townsend Jr, M.R. Hellmich, Gastrointestinal Hormone Receptors in Primary Human Colorectal Carcinomas1, Journal of Surgical Research 129(2) (2005) 313-321.
[22] J.-G. Zhang, J.-X. Liu, X.-X. Jia, J. Geng, F. Yu, B. Cong, Cholecystokinin octapeptide regulates the differentiation and effector cytokine production of CD4+ T cells in vitro, International Immunopharmacology 20(2) (2014) 307-315.
[23] J.-G. Zhang, B. Cong, X.-X. Jia, H. Li, Q.-X. Li, C.-L. Ma, Y. Feng, Cholecystokinin octapeptide inhibits immunoglobulin G1 production of lipopolysaccharide-activated B cells, International immunopharmacology 11(11) (2011) 1685-1690.
[24] J.-G. Zhang, B. Cong, Q.-X. Li, H.-Y. Chen, J. Qin, L.-H. Fu, Cholecystokinin octapeptide regulates lipopolysaccharide-activated B cells co-stimulatory molecule expression and cytokines production in vitro, Immunopharmacology and immunotoxicology 33(1) (2011) 157-163.
[25] E. von Guggenberg, P. Kolenc, C. Rottenburger, R. Mikołajczak, A. Hubalewska-Dydejczyk, Update on preclinical development and clinical translation of cholecystokinin-2 receptor targeting radiopharmaceuticals, Cancers 13(22) (2021) 5776.
[26] S. Kossatz, M. Béhé, R. Mansi, D. Saur, P. Czerney, W.A. Kaiser, I. Hilger, Multifactorial diagnostic NIR imaging of CCK2R expressing tumors, Biomaterials 34(21) (2013) 5172-5180.
[27] E. Laabs, M. Béhé, S. Kossatz, W. Frank, W.A. Kaiser, I. Hilger, Optical imaging of CCK2/gastrin receptor-positive tumors with a minigastrin near-infrared probe, Investigative Radiology 46(3) (2011) 196-201.
[28] R. Sun, Y. Wang, W. Shi, H. Zhang, J. Liu, W. He, Acidity-Triggered "Sticky Spotlight": CCK2R-Targeted TME-Sensitive NIR Fluorescent Probes for Tumor Imaging In Vivo, Bioconjugate Chemistry 35(4) (2024) 528-539.
[29] M. Konijnenberg, W. Breeman, O. Boerman, M. de Jong, Receptor occupancy constrains the radionuclide specific activity needed for tumour curability with radionuclide therapy more than the range of the beta-particles, Soc Nuclear Med, 2012.
[30] J. Sosabowski, C. Finucane, J. Foster, D. Ellison, J. Burnet, P. Laverman, S. Mather, Comparative small animal SPECT/CT imaging of twelve 111In-labelled CCK2-receptor targeting peptides, Soc Nuclear Med, 2011.
[31] P. Laverman, J. Sosabowski, L. Joosten, M. Cooper, J. Foster, J. Burnet, W. Oyen, P. Blower, S. Mather, O. Boerman, PET and SPECT imaging with a CCK2 receptor-binding peptide comparing various chelators and radionuclides, Soc Nuclear Med, 2013.
[32] P. Laverman, L. Joosten, A. Eek, S. Roosenburg, P.K. Peitl, T. Maina, H. Mäcke, L. Aloj, E. von Guggenberg, J.K. Sosabowski, Comparative biodistribution of 12 111 In-labelled gastrin/CCK2

receptor-targeting peptides, European journal of nuclear medicine and molecular imaging 38 (2011) 1410-1416.
[33] F. Schmitz, J.M. Otte, H. Stechele, B. Reimann, T. Banasiewicz, U. Fölsch, W. Schmidt, K.H. Herzig, CCK‐B/gastrin receptors in human colorectal cancer, European journal of clinical investigation 31(9) (2001) 812-820.
[34] M.D. Willard, M.E. Lajiness, I.H. Wulur, B. Feng, M.L. Swearingen, M.T. Uhlik, K.W. Kinzler, V.E. Velculescu, T. Sjöblom, S.D. Markowitz, Somatic mutations in CCK2R alter receptor activity that promote oncogenic phenotypes, Molecular Cancer Research 10(6) (2012) 739-749.
[35] Y. Song, Y. Xu, Z. Wang, Y. Chen, Z. Yue, P. Gao, C. Xing, H. Xu, MicroRNA‐148b suppresses cell growth by targeting cholecystokinin‐2 receptor in colorectal cancer, International journal of cancer 131(5) (2012) 1042-1051.
[36] D. Zhang, M. Jia, C. Wang, Y. Li, C. Ma, G. Zhu, R. Ma, D. Wen, X. Jia, G. Xu, CCK2-receptor deficiency impairs immune balance by influencing CD4+ T cells development by inhibiting cortical-thymic-epithelial-cells, Experimental Biology and Medicine 248(20) (2023) 1718-1731.